UNIVERSITÀ DELLA CALABRIA
DIMES
April 9 – 11, 2019

Introduction to Microwave Imaging Part II: Linear Inversion Methods

Natalia K. Nikolova
nikolova@ieee.org

McMaster University
Department of Electrical and Computer Engineering
Electromagnetic Vision (EMVi) Research Laboratory
Hamilton, ON CANADA

COURSE OVERVIEW

Day 1: Introduction & Forward Models of Microwave Imaging

- Field-based Integral Solutions of the Scattering Problem in Time and Frequency
- Born and Rytov Approximations of the Forward Model of Scattering
- Scattering Parameters and Integral Solutions in terms of *S*-parameters
- 2D Model of Tomography in Microwave Scattering

Day 2: Linear Inversion Methods

- Deconvolution Methods
  - Microwave Holography (MH)
  - Scattered Power Mapping (SPM)
- Image Reconstruction of Pulsed-radar Data
  - Synthetic Focusing: Delay and Sum (DAS)

Day 3: Performance Metrics & Hardware

- Spatial Resolution
- Dynamic Range
- Data Signal-to-noise Ratio

Select Topics

- Overview of Nonlinear Inversion Methods
  - Direct Iterative Methods
  - Model-based Optimization Methods
- Tissue Imaging – Challenges and Advancements

THE KERNEL OF THE DATA EQUATION: POINT-SPREAD FUNCTION (PSF)

THE REALISTIC MEASUREMENT SCENARIO

- microwave measurements involve scanning over large acquisition surfaces – each response being function of the observation position **r**
- at each observation position **r** several responses may be acquired

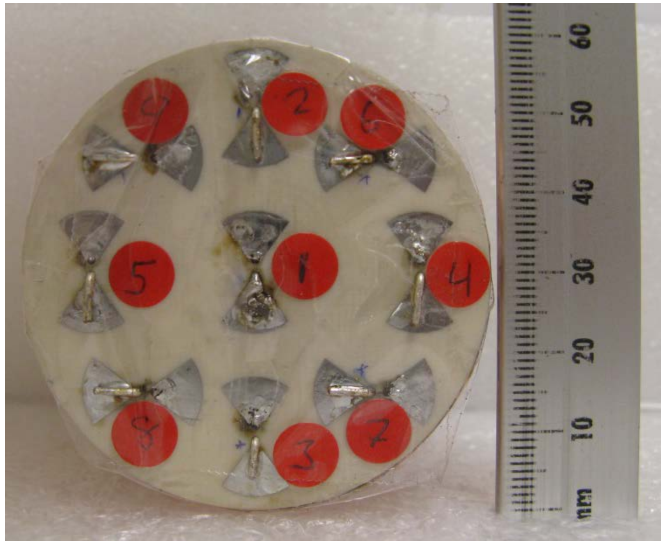
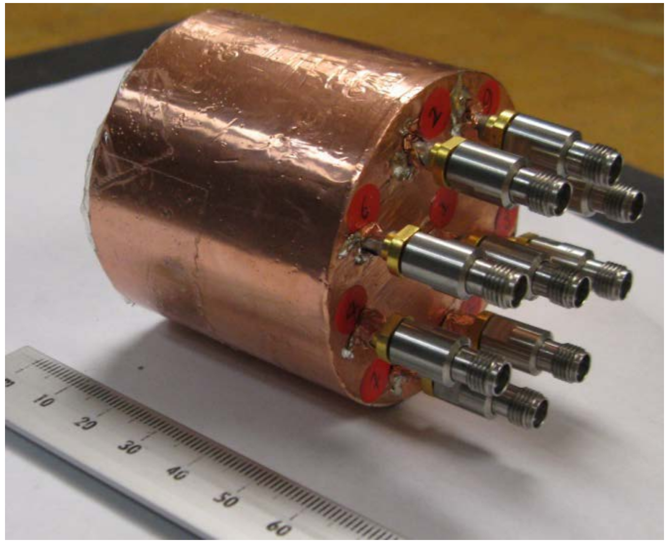

example of antenna array measuring 9 responses at each **r**

[Amineh et al., *IEEE Trans. Instr. Meas.*, 2015][Photo credit: Justin J. McCombe]

THE REALISTIC MEASUREMENT SCENARIO: PLANAR SCANNING

- example of planar scanning for microwave imaging

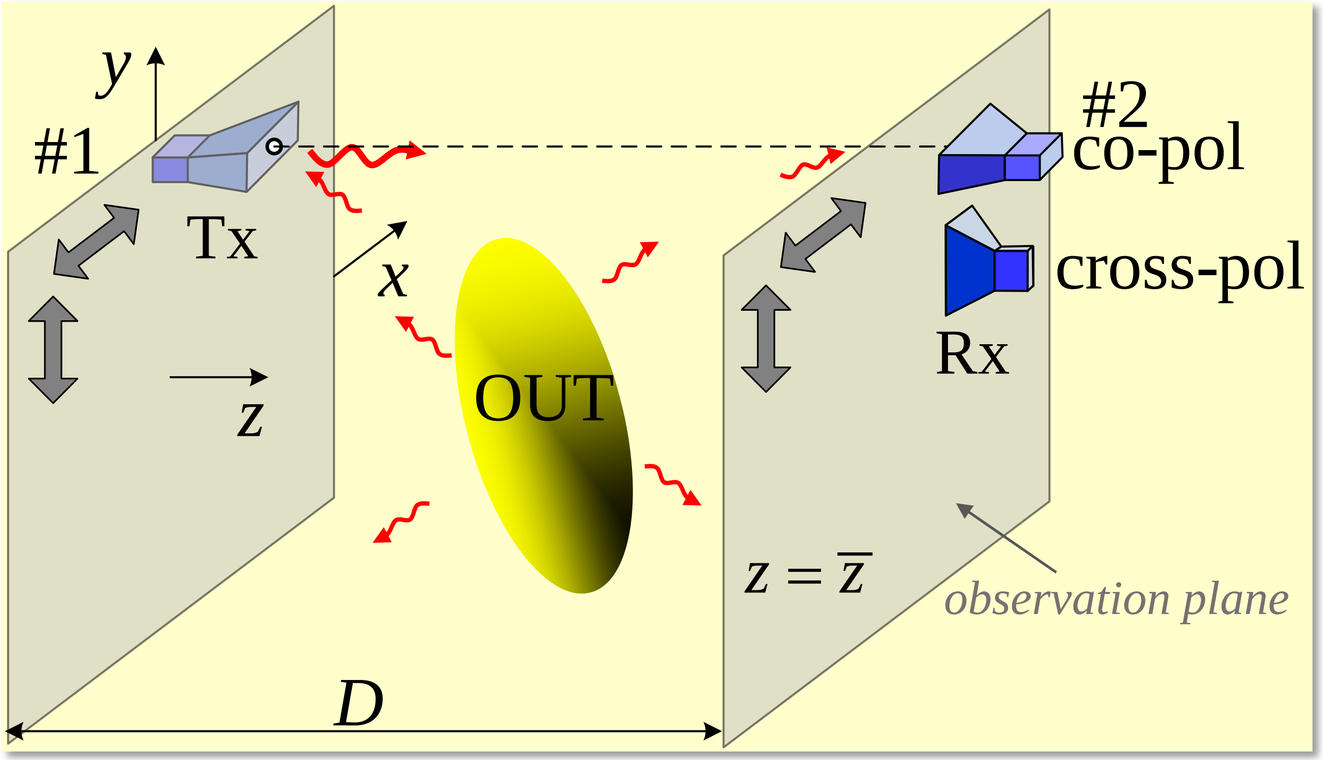

type of response	number of values $S_{ik}(x,y)$
co-pol X-X	$4xN_\omega$
co-pol Y-Y	$4xN_\omega$
cross-pol X-Y	$4xN_\omega$
cross-pol Y-X	$4xN_\omega$
TOTAL	$16xN_\omega$

number of possible responses acquired at each position

- reflected signals: S_{11}, S_{22}
- transmitted signals: S_{21}, S_{12} ($S_{21} = S_{12}$ in reciprocal systems)

FORWARD MODEL WITH PLANAR SCANNING

- S-parameter forward model in planar scanning

$$\underbrace{S_{\xi}^{\mathrm{sc}}(x,y,\bar{z};\omega)}_{\text{data}} \approx \frac{\mathrm{i}\omega\varepsilon_0}{\underbrace{2a_i a_k}_{\kappa}} \iiint_{V_s} \Delta\varepsilon_{\mathrm{r}}(x',y',z') \left[\mathbf{E}_{\xi,\mathrm{Rx}}^{\mathrm{inc}} \cdot \mathbf{E}_{\xi,\mathrm{Tx}}^{\mathrm{inc}} \right]_{(x',y',z';x,y,\bar{z};\omega)} dx'dy'dz', \ \xi = 1,\ldots,N_T$$

- ξ (response type) replaces (i,k)

EXAMPLE: RESPONSE TYPES WITH 2-PORT MEASUREMENT

ξ	(i,k)	**response type**
1	(1,1)	reflection S_{11}
2	(2,2)	reflection S_{22}
3	(1,2) or (2,1)	transmission $S_{12} = S_{21}$

$N_T = 3$

FORWARD MODEL WITH PLANAR SCANNING – 2

- S-parameter forward model in planar scanning

$$S_{\xi}^{\mathrm{sc}}(\underbrace{x, y, \bar{z}}_{\mathbf{r}_{\mathrm{Rx}} \& \mathbf{r}_{\mathrm{Tx}}};\omega) \approx \kappa \iiint_{V_s} \Delta\varepsilon_{\mathrm{r}}(x', y', z') \left[\mathbf{E}_{\xi,\mathrm{Rx}}^{\mathrm{inc}} \cdot \mathbf{E}_{\xi,\mathrm{Tx}}^{\mathrm{inc}} \right]_{(x',y',z';x,y,\bar{z};\omega)} dx'dy'dz', \ \xi = 1,\ldots,N_T$$

- position of Tx/Rx antenna pair given by $\mathbf{r}_{\mathrm{Rx}}$

$$\mathbf{r}_{\mathrm{Rx}} \equiv (x, y, \bar{z}) \text{ and } \mathbf{r}_{\mathrm{Tx}} \equiv (x, y, \bar{z} - D)$$

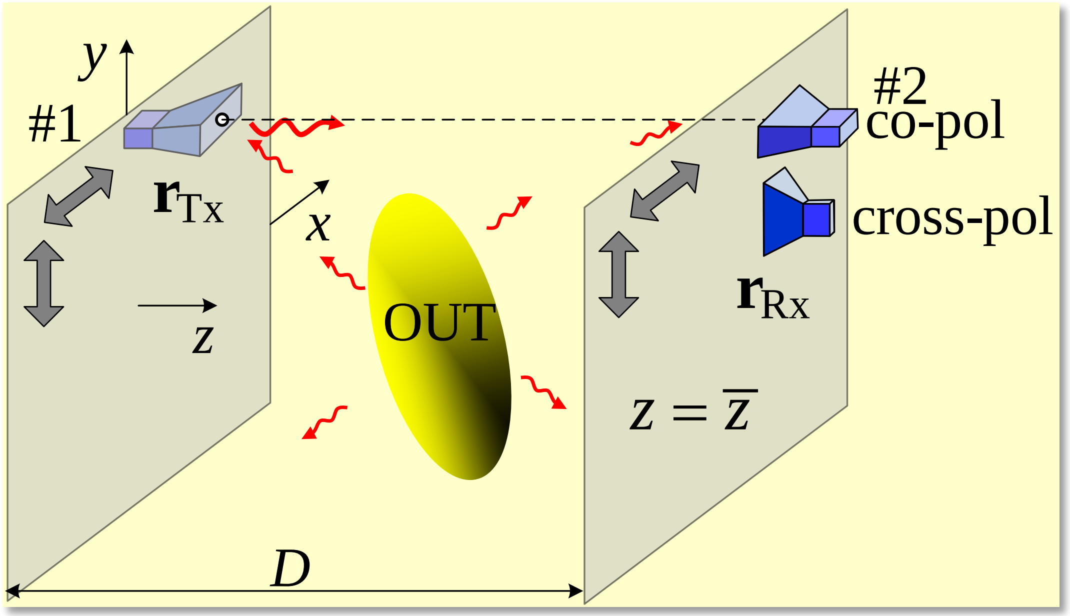

FORWARD MODEL: OBTAINING THE RESOLVENT KERNEL

- resolvent kernel of forward model – re-visiting last lecture

$$S_\xi^{\mathrm{sc}}(x,y,\bar{z};\omega) \approx \kappa \iiint_{V_\mathrm{s}} \Delta\varepsilon_\mathrm{r}(x',y',z') \underbrace{\left[\bar{\mathbf{E}}_{\xi,\mathrm{Rx}}^{\mathrm{inc}} \cdot \bar{\mathbf{E}}_{\xi,\mathrm{Tx}}^{\mathrm{inc}}\right]_{(x',y',z';x,y,\bar{z};\omega)}}_{\text{approximate (Born) resolvent kernel } \mathcal{K}_\xi(\mathbf{r}';\mathbf{r};\omega)} dx'dy'dz',\ \xi = 1,\ldots,N_T$$

- method 1: analytical far-zone expressions well suited only for measurements in air with large stand-off distances

- method 2: simulated field distributions suffer from *modeling errors*

- method 3: **Measurements? Yes, measure the system point-spread function (PSF)**

[Savelyev&Yarovoy, *EuRAD* 2012][Amineh *et al.*, *IEEE Trans. Instrum. Meas.*, 2015]

RESOLVENT KERNEL & POINT-SPREAD FUNCTION (PSF)

- PSF is data measured with point scatterer (electrically small object)

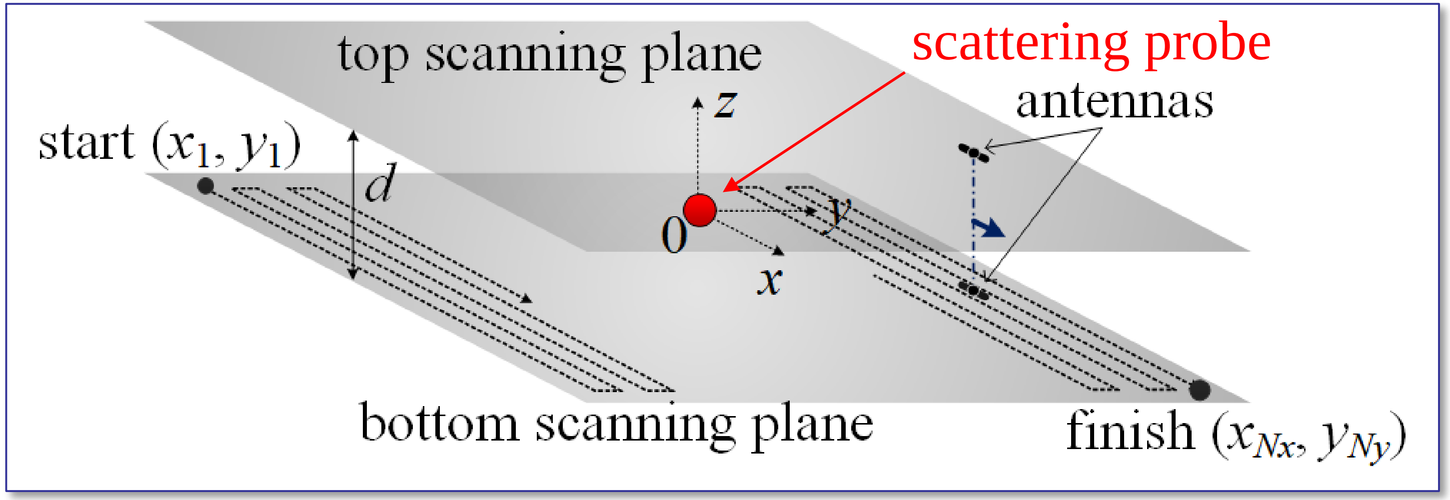

- relating PSF to kernel

$$S_\xi^{\mathrm{PSF}}(x,y,\bar{z};\omega) \approx \kappa \iiint_{V_s} \underbrace{\Delta\varepsilon_{\mathrm{r,sp}} \delta(x-x', y-y', z-z')}_{\text{scattering probe (sp) contrast}} \cdot \mathcal{K}_\xi(x',y',z';x,y,\bar{z};\omega)\,dx'dy'dz'$$

$$\Rightarrow S_\xi^{\mathrm{PSF}}(x,y,\bar{z};x',y',z';\omega) \approx \underbrace{\left(\kappa \Delta\varepsilon_{\mathrm{r,sp}} \Omega_{\mathrm{sp}}\right)}_{\text{known constants}} \cdot \mathcal{K}_\xi(x',y',z';x,y,\bar{z};\omega),\ \xi = 1,\ldots,N_T$$

RESOLVENT KERNEL & POINT-SPREAD FUNCTION (PSF) – 2

$$\mathcal{K}_\xi(x',y',z';x,y,\overline{z};\omega)=\frac{S_\xi^{\mathrm{PSF}}(x,y,\overline{z};x',y',z';\omega)}{\kappa\Delta\varepsilon_{\mathrm{r,sp}}\Omega_{\mathrm{sp}}},\ \xi=1,\ldots,N_T$$

- notice the simple exchange of positions allowing to obtain the kernel from the PSF

$$\mathcal{K}_\xi(\mathbf{r}';\mathbf{r};\omega)=\frac{S_\xi^{\mathrm{PSF}}(\mathbf{r};\mathbf{r}';\omega)}{\kappa\Delta\varepsilon_{\mathrm{r,sp}}\Omega_{\mathrm{sp}}}$$

observation: $\mathbf{r}\equiv(x,y,z)$
integration (probe location): $\mathbf{r}'\equiv(x',y',z')$

- if medium in V_{s} is uniform (or layered for planar acquisition) – probe needs to be measured only at the center of an imaged plane $z'=const$

measured centered PSF: $S_{\xi,0}^{\mathrm{PSF}}(x,y,\overline{z};z';\omega)\equiv S_\xi^{\mathrm{PSF}}(x,y,\overline{z};0,0,z';\omega)$

RESOLVENT KERNEL & POINT-SPREAD FUNCTION (PSF) – 3

- since medium is uniform or layered

$$S_\xi^{\text{PSF}}(x,y,\overline{z};x',y',z';\omega) = S_{\xi,0}^{\text{PSF}}(x-x',y-y',\overline{z};z';\omega) \longleftarrow$$

probe moves left/right →
response moves left/right

$$\mathcal{K}_\xi(x',y',z';x,y,\overline{z};\omega) = \frac{S_{\xi,0}^{\text{PSF}}(x-x',y-y',\overline{z};z';\omega)}{\kappa\Delta\varepsilon_{\text{r,sp}}\Omega_{\text{sp}}}, \; \xi = 1,\ldots,N_T$$

$$\Rightarrow S_\xi^{\text{sc}}(x,y,\overline{z};\omega) \approx \frac{1}{\Delta\varepsilon_{\text{r,sp}}\Omega_{\text{sp}}} \iiint_{V_s} \underbrace{\Delta\varepsilon_{\text{r}}(x',y',z') S_{\xi,0}^{\text{PSF}}(x-x',y-y',\overline{z};z';\omega)}_{\text{convolution in } x,y} dx'dy'dz', \; \xi = 1,\ldots,N_T$$

- the measured response is a convolution of the contrast and the system PSF
- the image reconstruction can then be viewed as a de-convolution process!

[Tajik *et al.*, *JPIER- B*, 2017][Shumakov *et al.*, *Trans. MTT*, 2018]

- system calibration involves two measurements:
  (i) reference object (RO) – incident-field data
  (ii) calibration object (CO) – scattering-probe data

- PSF extraction

➢ Born Method

$$S_{\xi 0}^{\mathrm{PSF}}(\cdot) \approx \left(S_{\xi 0}^{\mathrm{PSF}}(\cdot)\right)_{\mathrm{B}} = S_{\xi}^{\mathrm{CO}}(\cdot) - S_{\xi}^{\mathrm{RO}}(\cdot)$$

➢ Rytov Method

$$S_{\xi 0}^{\mathrm{PSF}}(\cdot) \approx \left(S_{\xi 0}^{\mathrm{PSF}}(\cdot)\right)_{\mathrm{R}} = S_{\xi}^{\mathrm{RO}}(\cdot) \ln\left(\frac{S_{\xi}^{\mathrm{CO}}(\cdot)}{S_{\xi}^{\mathrm{RO}}(\cdot)}\right)$$

$$(\cdot) \equiv (x, y, \overline{z}; \omega), \;\; \xi = 1, \ldots, N_T$$

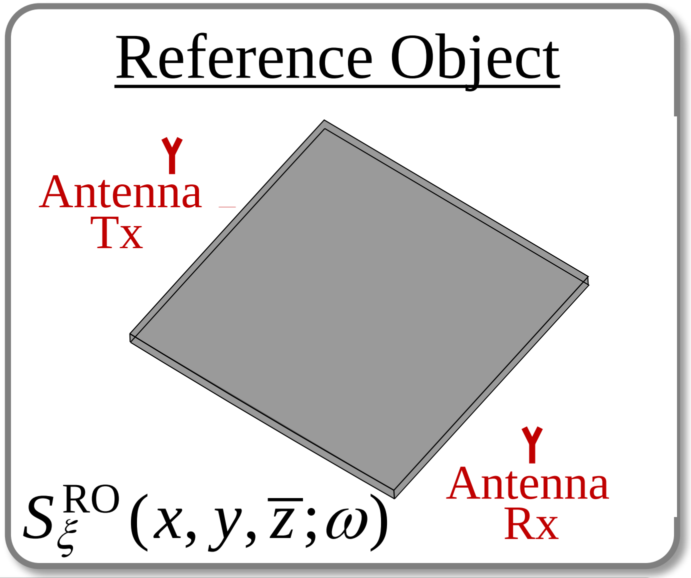

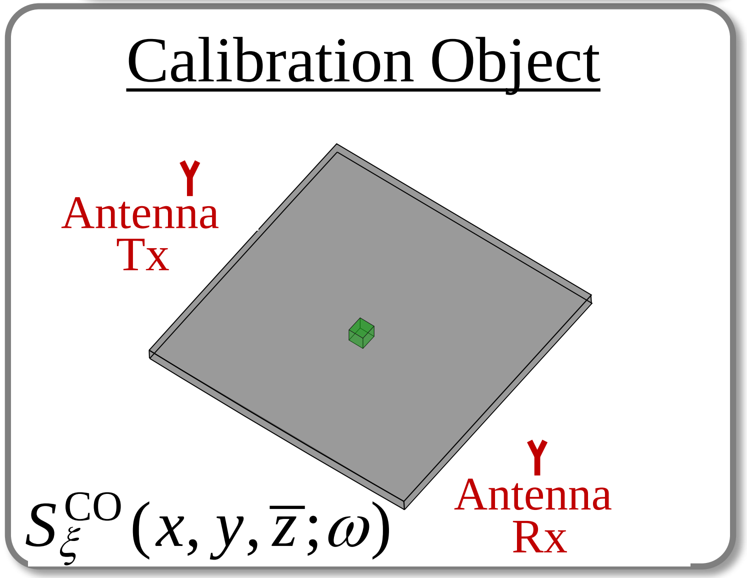

EXAMPLE: PSF

- typical noise-free PSF obtained from simulated RO and CO data

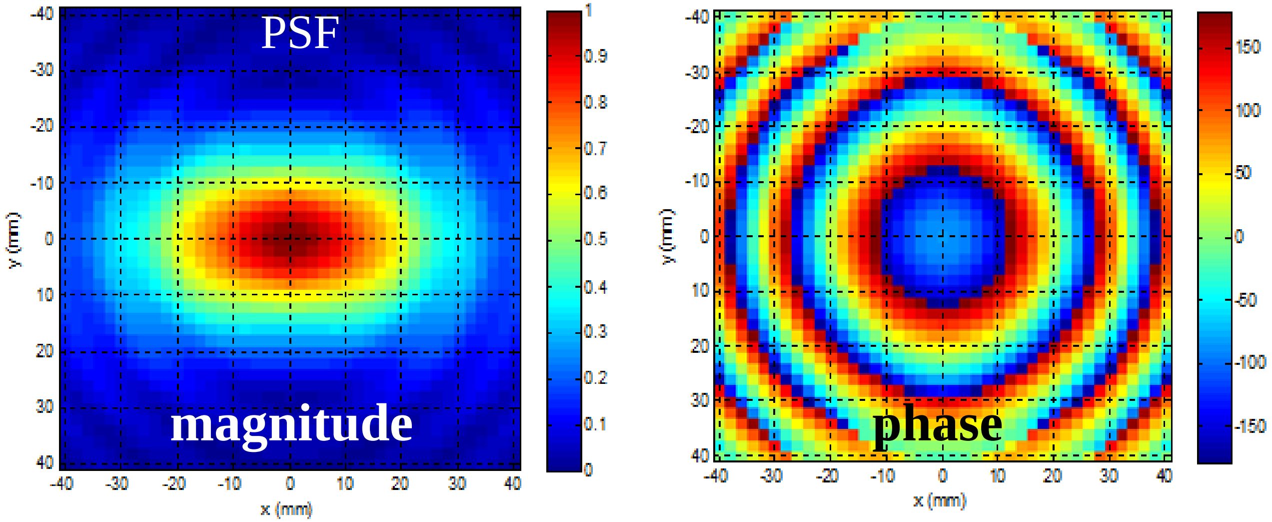

$\boxed{f = 6.5 \text{ GHz}}$

[Amineh *et al.*, *IEEE Trans. Instrum. Meas.*, 2015]

- typical noisy PSF obtained from measurements (magnitude shown) **[Tajik *et al.*, *EuCAP 2019*]**

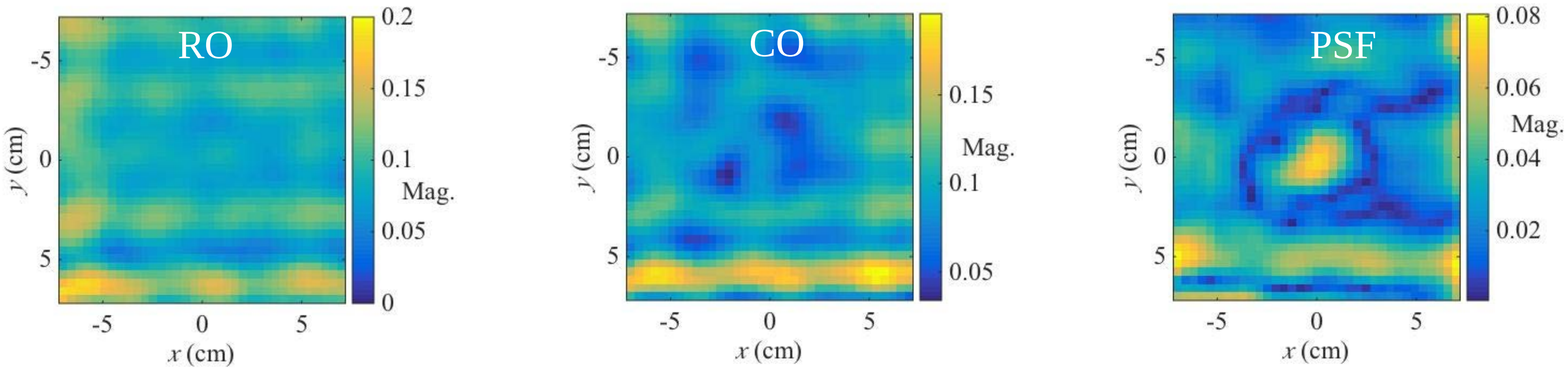

MEASUREMENT PROCEDURE: DATA EXTRACTION

- data is extracted with the same method as that for PSF – being consistent is important!

➢ Born Method

$$S_{\xi}^{\text{sc}}(\cdot) \approx \left(S_{\xi}^{\text{sc}}(\cdot)\right)_{\text{B}} = S_{\xi}^{\text{OUT}}(\cdot) - S_{\xi}^{\text{RO}}(\cdot)$$

➢ Rytov Method

$$S_{\xi}^{\text{sc}}(\cdot) \approx \left(S_{\xi}^{\text{sc}}(\cdot)\right)_{\text{R}} = S_{\xi}^{\text{RO}}(\cdot) \ln\left(\frac{S_{\xi}^{\text{OUT}}(\cdot)}{S_{\xi}^{\text{RO}}(\cdot)}\right)$$

$$(\cdot) \equiv (x, y, \overline{z}; \omega), \;\; \xi = 1, \ldots, N_T$$

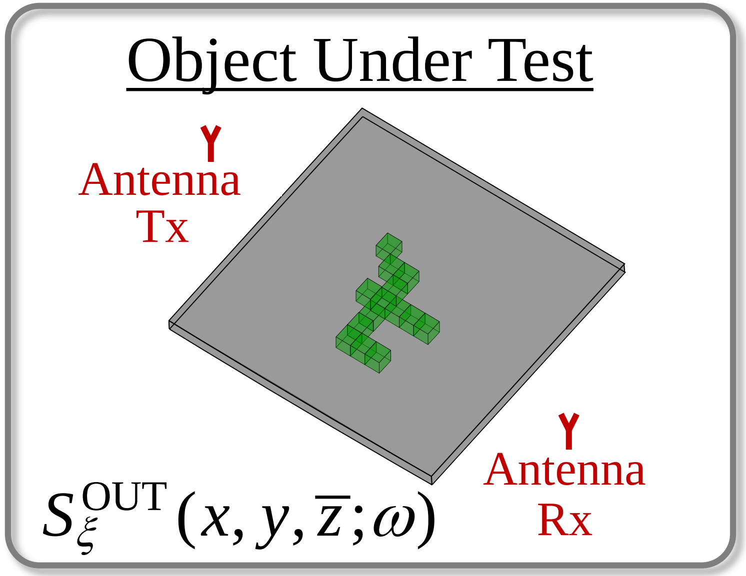

INVERSION WITH MICROWAVE HOLOGRAPHY

DATA EQUATION IN FOURIER SPACE

$$S_\xi^{\mathrm{sc}}(x,y,\bar{z};\omega) \approx \frac{1}{\Delta\varepsilon_{\mathrm{r,sp}}\Omega_{\mathrm{sp}}} \int_{x'}\int_{y'}\int_{z'} \Delta\varepsilon_{\mathrm{r}}(x',y',z') S_{\xi,0}^{\mathrm{PSF}}(x-x',y-y',\bar{z};z';\omega)\, dx'dy'dz',\ \xi = 1,\ldots,N_T$$

$\Downarrow$ 2D FT

- in Fourier (or k) space

$$\tilde{S}_\xi(k_x,k_y;\bar{z};\omega) \approx \frac{\Delta x'\Delta y'}{\Delta\varepsilon_{\mathrm{r,sp}}\Omega_{\mathrm{sp}}} \int_{z'} \underbrace{\tilde{F}(k_x,k_y;z')}_{\mathrm{FT_{2D}}\{\Delta\varepsilon_{\mathrm{r}}(x',y',z')\}} \cdot \tilde{S}_{\xi,0z'}^{\mathrm{PSF}}(k_x,k_y;z';\omega)\, dz'$$

- discretize integral along z' into a sum
- we now have a system of equations to solve ***at each spectral position*** $\boldsymbol{\kappa} = (k_x, k_y)$

$$\tilde{S}_\xi^{(m)}(\boldsymbol{\kappa}) \approx \sum_{n=1}^{N_z} \tilde{f}(\boldsymbol{\kappa};z'_n)\left[\tilde{S}_{\xi,0}^{\mathrm{PSF}}(\boldsymbol{\kappa};z'_n)\right]^{(m)} \quad \begin{array}{l} m = 1,\ldots,N_\omega \\ \xi = 1,\ldots,N_T \end{array}$$

$$\tilde{f}(\boldsymbol{\kappa};z'_n) = \frac{\overbrace{\boxed{\Delta x'\Delta y'\Delta z'_n}}^{\Omega_{\mathrm{v}}}}{\Delta\varepsilon_{\mathrm{r,sp}}\Omega_{\mathrm{sp}}} \cdot \tilde{F}(\boldsymbol{\kappa};z'_n)$$

INVERSION IN FOURIER SPACE

$$\underbrace{\tilde{S}_{\xi}^{(m)}(\boldsymbol{\kappa})}_{\text{data } \boldsymbol{d}(\boldsymbol{\kappa})} \approx \sum_{n=1}^{N_z} \underbrace{\tilde{f}(\boldsymbol{\kappa}; z'_n)}_{\text{contrast } \boldsymbol{f}(\boldsymbol{\kappa})} \underbrace{\left[\tilde{S}_{\xi,0z'}^{\text{PSF}}(\boldsymbol{\kappa}; z'_n)\right]^{(m)}}_{\text{system matrix } \boldsymbol{A}(\boldsymbol{\kappa})} \qquad \begin{array}{l} m = 1,\ldots,N_\omega \\ \xi = 1,\ldots,N_T \end{array}$$

in discrete Fourier space

$$\boldsymbol{\kappa}_{ij} \equiv (i\Delta k_x, j\Delta k_y)$$

- at each discrete point in Fourier space, a small system of equations is solved for a total of $N_x N_y$ such systems

$$\boldsymbol{A}(\boldsymbol{\kappa}_{ij}) \cdot \boldsymbol{f}(\boldsymbol{\kappa}_{ij}) = \boldsymbol{d}(\boldsymbol{\kappa}_{ij}) \quad i = 1,\ldots,N_x, \quad j = 1,\ldots,N_y$$

$\Downarrow$

vectors of response types

$$[\tilde{\boldsymbol{S}}^{(m)}(\cdot)]^T = \left[\tilde{S}_1^{(m)}(\cdot) \ \cdots \ \tilde{S}_{N_T}^{(m)}(\cdot)\right]$$

$$\begin{bmatrix} \left[\tilde{\boldsymbol{S}}_0^{\text{PSF}}(\boldsymbol{\kappa}_{ij}; z'_1)\right]^{(1)} & \cdots & \left[\tilde{\boldsymbol{S}}_0^{\text{PSF}}(\boldsymbol{\kappa}_{ij}; z'_{N_z})\right]^{(1)} \\ \vdots & \ddots & \vdots \\ \left[\tilde{\boldsymbol{S}}_0^{\text{PSF}}(\boldsymbol{\kappa}_{ij}; z'_1)\right]^{(N_\omega)} & \cdots & \left[\tilde{\boldsymbol{S}}_0^{\text{PSF}}(\boldsymbol{\kappa}_{ij}; z'_{N_z})\right]^{(N_\omega)} \end{bmatrix}_{N_\omega N_T \times N_z} \cdot \begin{bmatrix} \tilde{f}(\boldsymbol{\kappa}_{ij}; z'_1) \\ \vdots \\ \tilde{f}(\boldsymbol{\kappa}_{ij}; z'_{N_z}) \end{bmatrix}_{N_z \times 1} = \begin{bmatrix} \tilde{\boldsymbol{S}}^{(1)}(\boldsymbol{\kappa}_{ij}) \\ \vdots \\ \tilde{\boldsymbol{S}}^{(N_\omega)}(\boldsymbol{\kappa}_{ij}) \end{bmatrix}_{N_\omega N_T \times 1}$$

FINAL STEP: BACK TO X-Y SPACE

- at each plane along range (z'_n, $n = 1, \ldots, N_z$)

$$\Delta\varepsilon_{\mathrm{r}}(x', y', z'_n) = \frac{\Delta\varepsilon_{\mathrm{r,sp}}\Omega_{\mathrm{sp}}}{\Omega_{\mathrm{v}}} \mathcal{F}_{\mathrm{2D}}^{-1}\left\{ \tilde{f}(\boldsymbol{\kappa}; z'_n) \right\},\ n = 1, \ldots, N_z$$

$$\varepsilon_{\mathrm{r}}(x', y', z'_n) = \varepsilon_{\mathrm{r,b}} + \Delta\varepsilon_{\mathrm{r}}(x', y', z'_n)$$

ADVANTAGES OF SOLVING IN FOURIER SPACE: *DIVIDE AND CONQUER*

- we solve ($N_x \cdot N_y$) small systems of equations
  number of solved systems on the order of 10^4 to 10^5

- size of each system is small: $N_T N_\omega \times N_z$ (e.g. 60×5)

- typical execution times: 2 to 3 seconds on a laptop using Matlab

- **solution is orders of magnitude faster than solving in real space** where one very large system of equations needs to be solved of size

$$N_D \times N_\mathrm{v} \text{ with } N_D = N_x N_y N_\omega N_T \sim 10^7 \text{ to } 10^8$$
$$N_\mathrm{v} = N_x N_y N_z \sim 10^6 \text{ to } 10^7$$

3-D SIMULATION EXAMPLE: C-shape and 3 Cubes

[Tajik *et al.*, *JPIER*-B 2017]

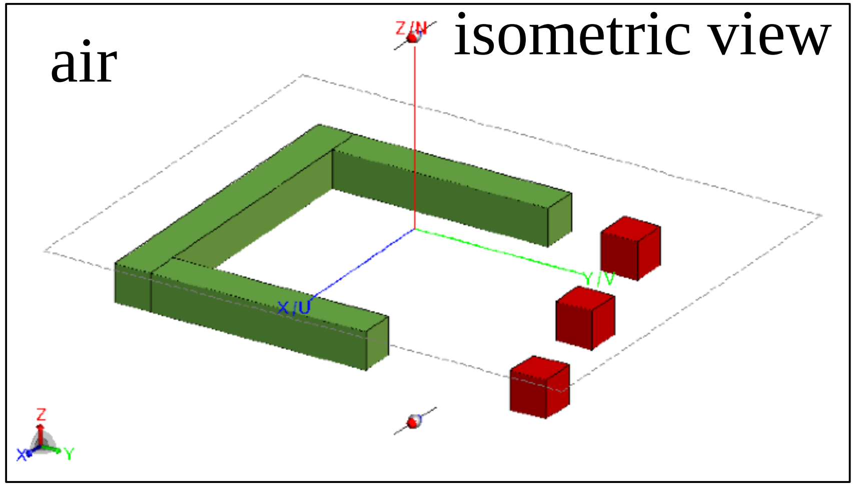

Object	ε_r
C-shape	1.5 - i0
Cubes	1.1 – i0

- 2 dipole antennas aligned along boresight, separated by 10 cm
- reflection and transmission coefficients acquired

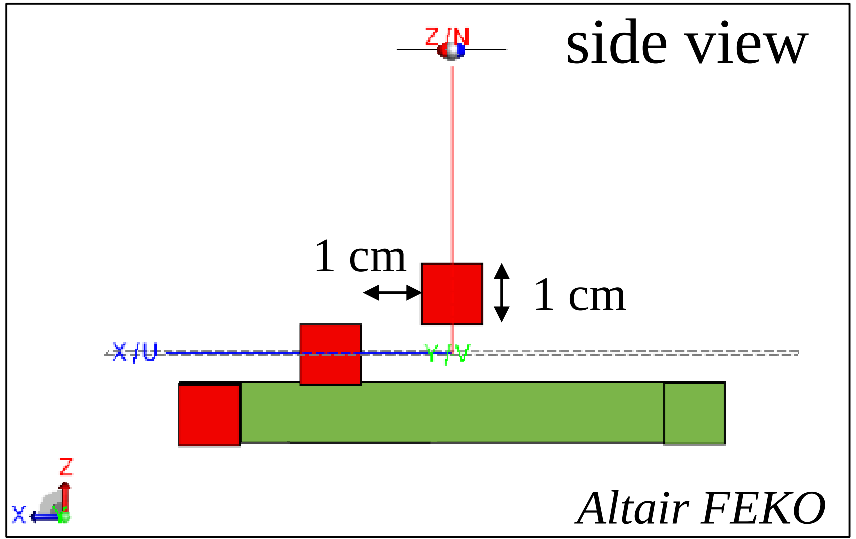

- C-shape is 4 cm from lower dipole
- cubes are 4 cm, 5 cm, and 6 cm from lower dipole
- acquisition plane of area 30 cm by 30 cm with 1 cm sampling interval along *x* and *y*
- frequency range from 3 GHz to 8 GHz, Δf = 1 GHz
- scattering probe in calibration: 1 cm^3 cube of $\varepsilon_{r,sp}$ = 1.1 – i0

3-D SIMULATION EXAMPLE: IMAGES OF C-shape and 3 Cubes

[Tajik *et al.*, *JPIER*-B 2017]

Born Approximation

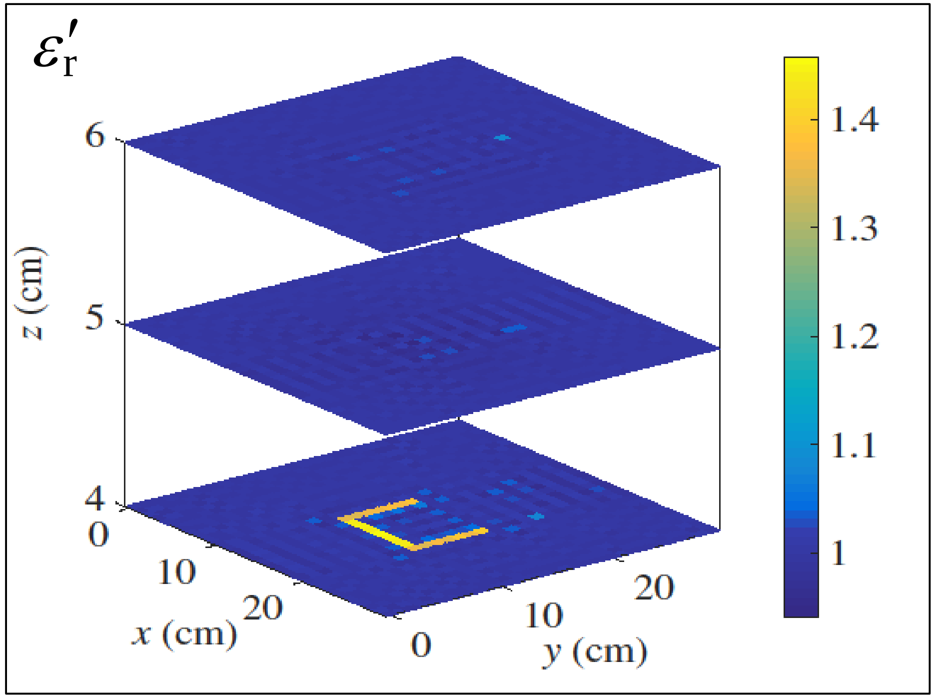

Rytov Approximation

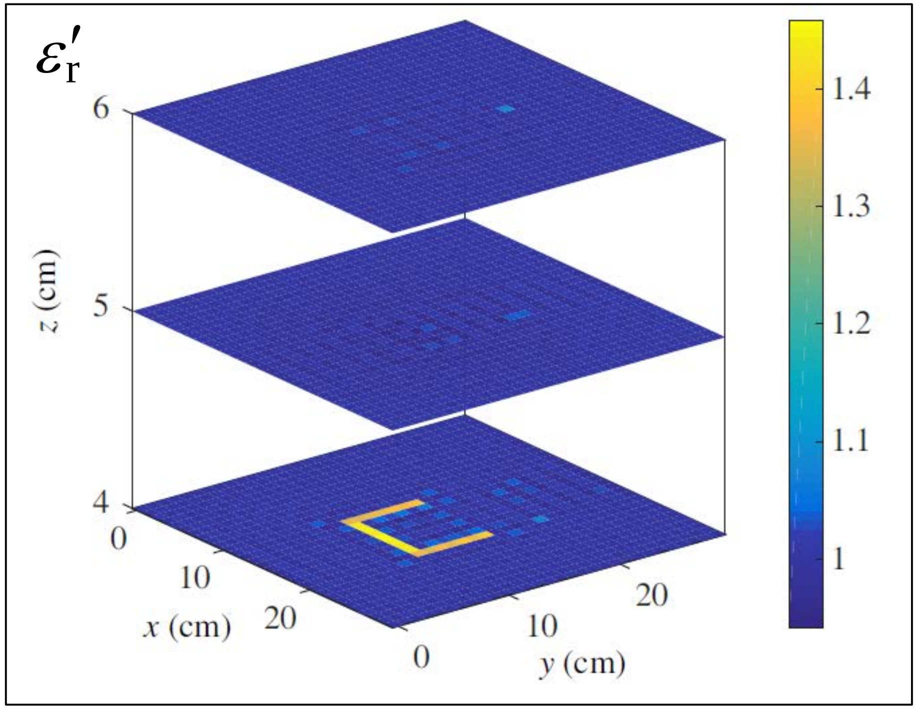

- due to the targets' low contrast, both approximation yield practically the same images
- quantitative estimate of permittivity distribution is very good

MEASUREMENT EXAMPLE: Teddy Bear (2-D Image)

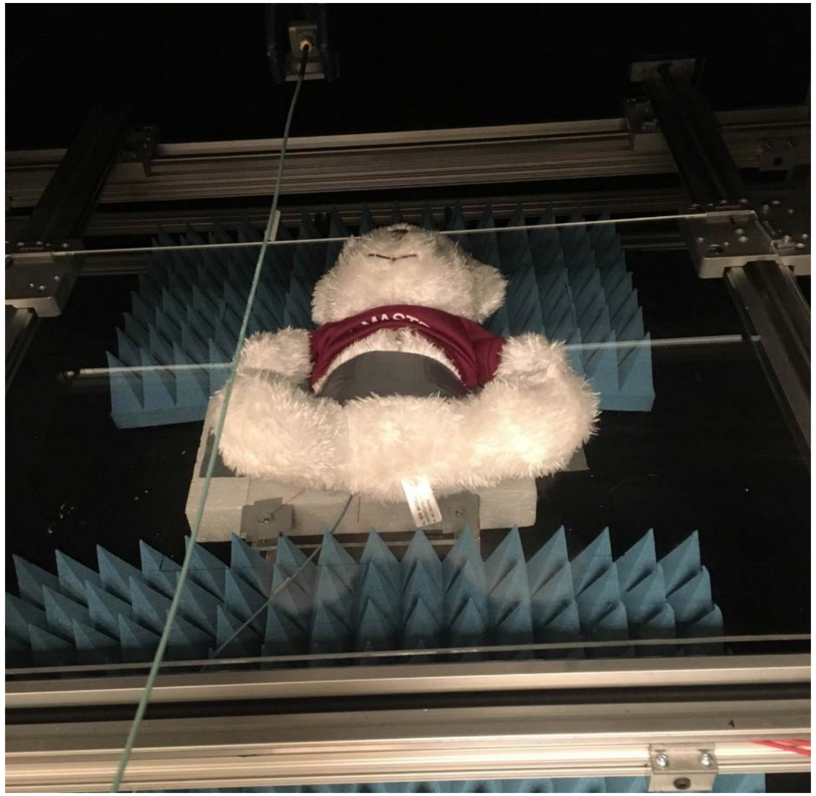

- scanned area: 29 cm by 29 cm
- sampling step along x and y: 5 mm
- only transmission coefficient acquired
- frequency range from 8 GHz to 12 GHz (41 samples)
- two open-end waveguides (WR-90) aligned along boresight
  - ➢ measurement 1: just teddy bear
  - ➢ measurement 2: two objects inserted in teddy bear

1) dielectric cross: $\varepsilon_r = 12 - i0$ (thickness 1 cm, cross arm 3 cm) inserted in bear's tummy
2) dielectric L-shaped object: $\varepsilon_r = 10 - i5$ (thickness 1 cm, L arm 2 cm) inserted in right arm

MEASUREMENT EXAMPLE: 2-D IMAGES OF Teddy Bear

normalized contrast

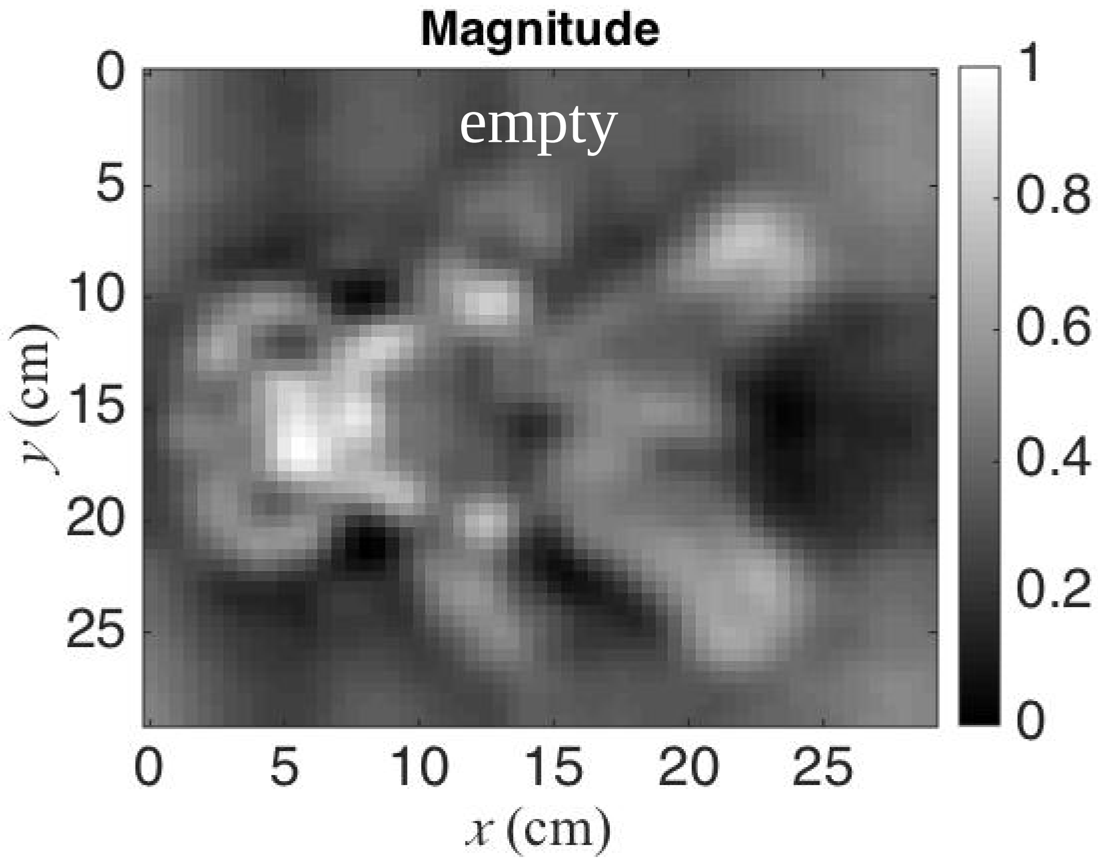

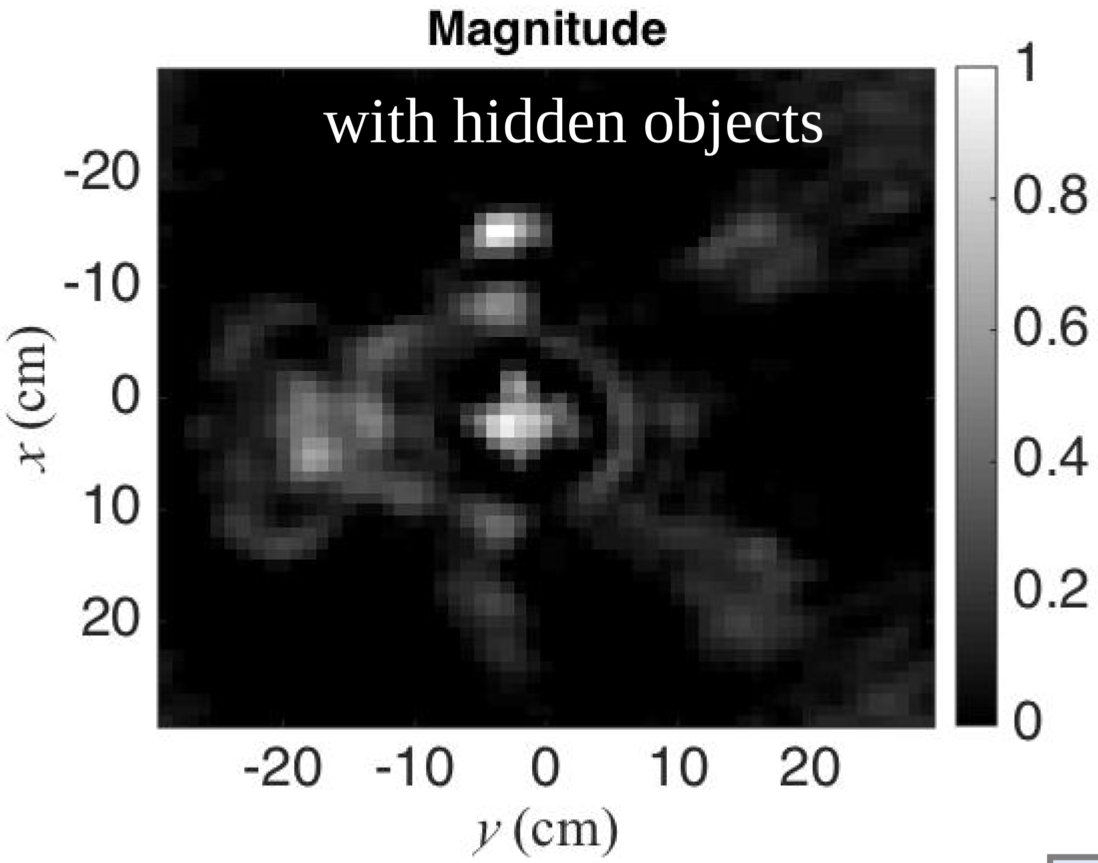

MEASUREMENT EXAMPLE: 2-D QUANTITATIVE ESTIMATES (Teddy Bear)

permittivity

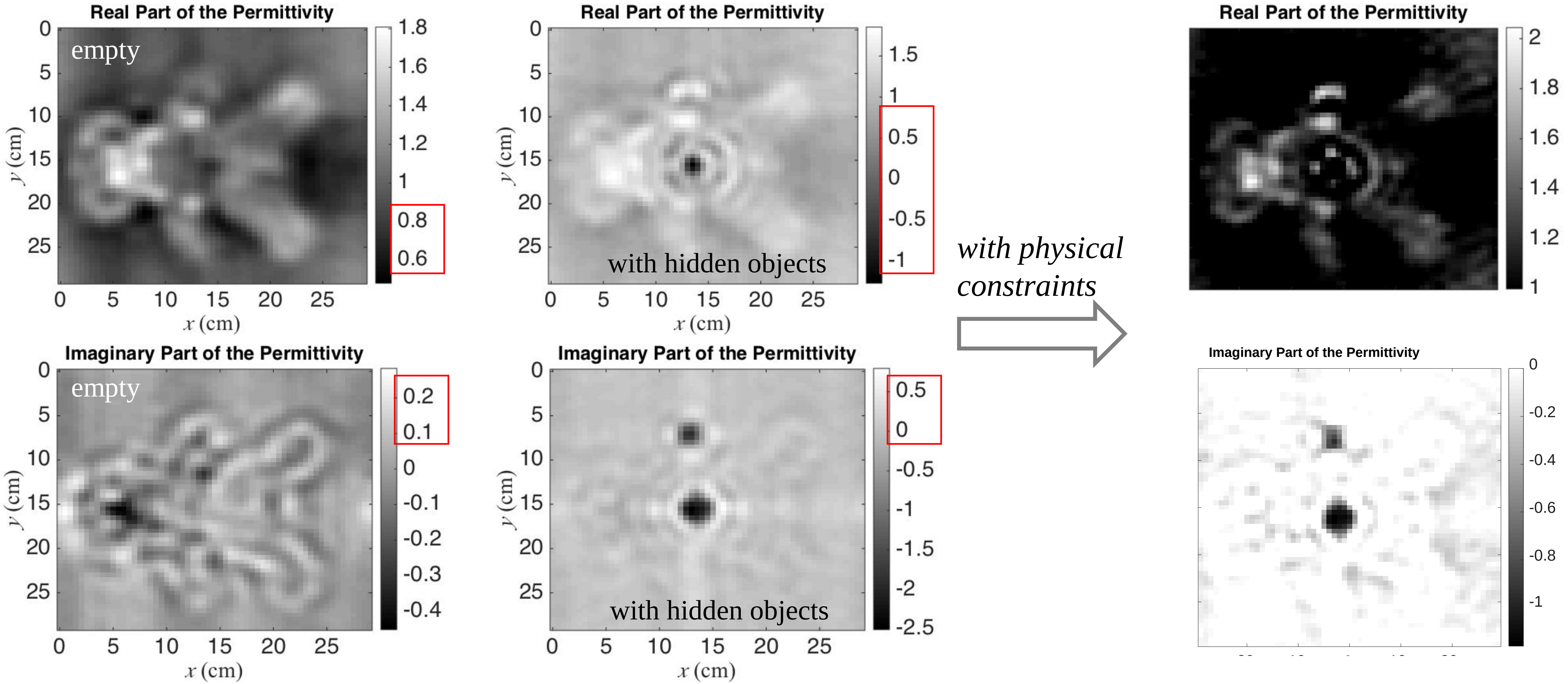

EXAMPLE: 3-D NEAR-ZONE IMAGING OF METALLIC OBJECTS (RE-VISITED)

[Amineh *et al.*, *Trans. IM*, 2015]

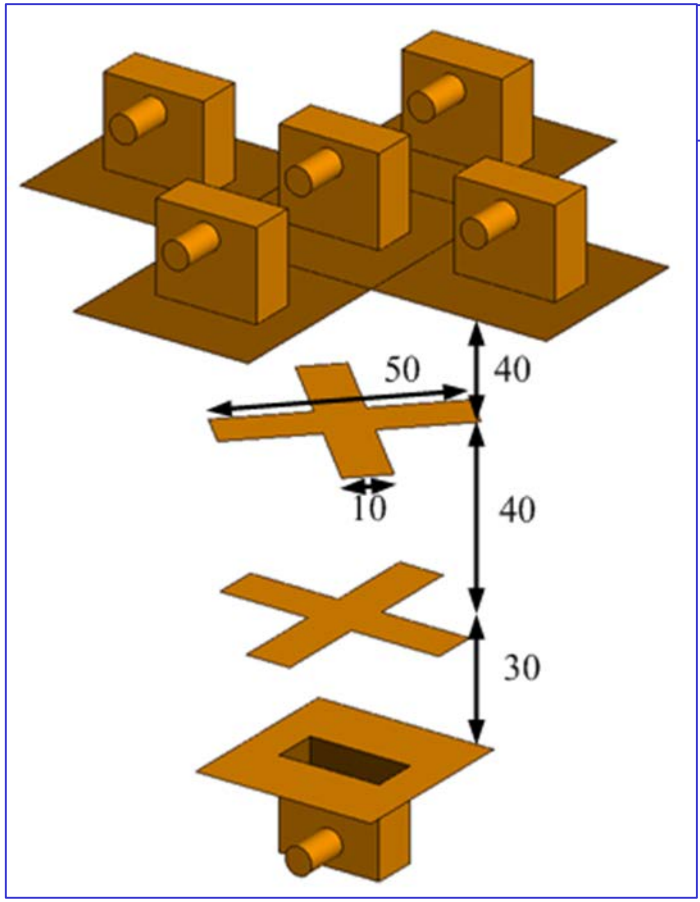

$$\Delta x = \Delta y = 5\,\text{mm}$$
$$\Delta f = 250\,\text{MHz}$$

f (GHz)	λ (mm)	D_{far} (mm)
3	100	12.5
8.2	37	34
20	15	83

X-band (WR90) open-end waveguides ($f_c \approx 6.56\,\text{GHz}$)

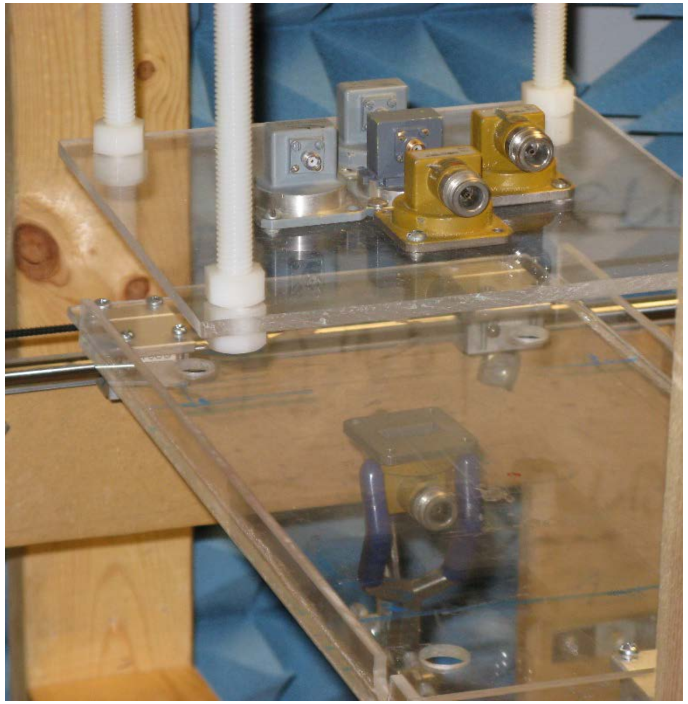

[photo credit: Justin McCombe]

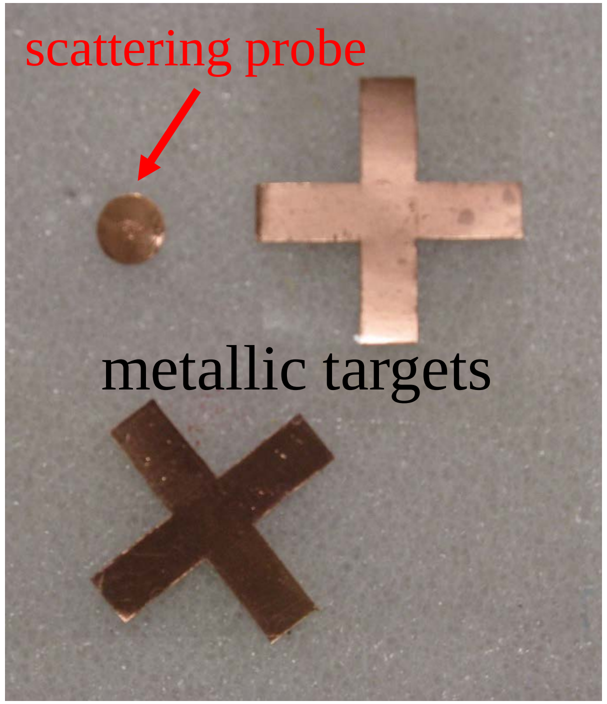

EXAMPLE: 3-D NEAR-ZONE IMAGING OF METALLIC OBJECTS (RE-VISITED)

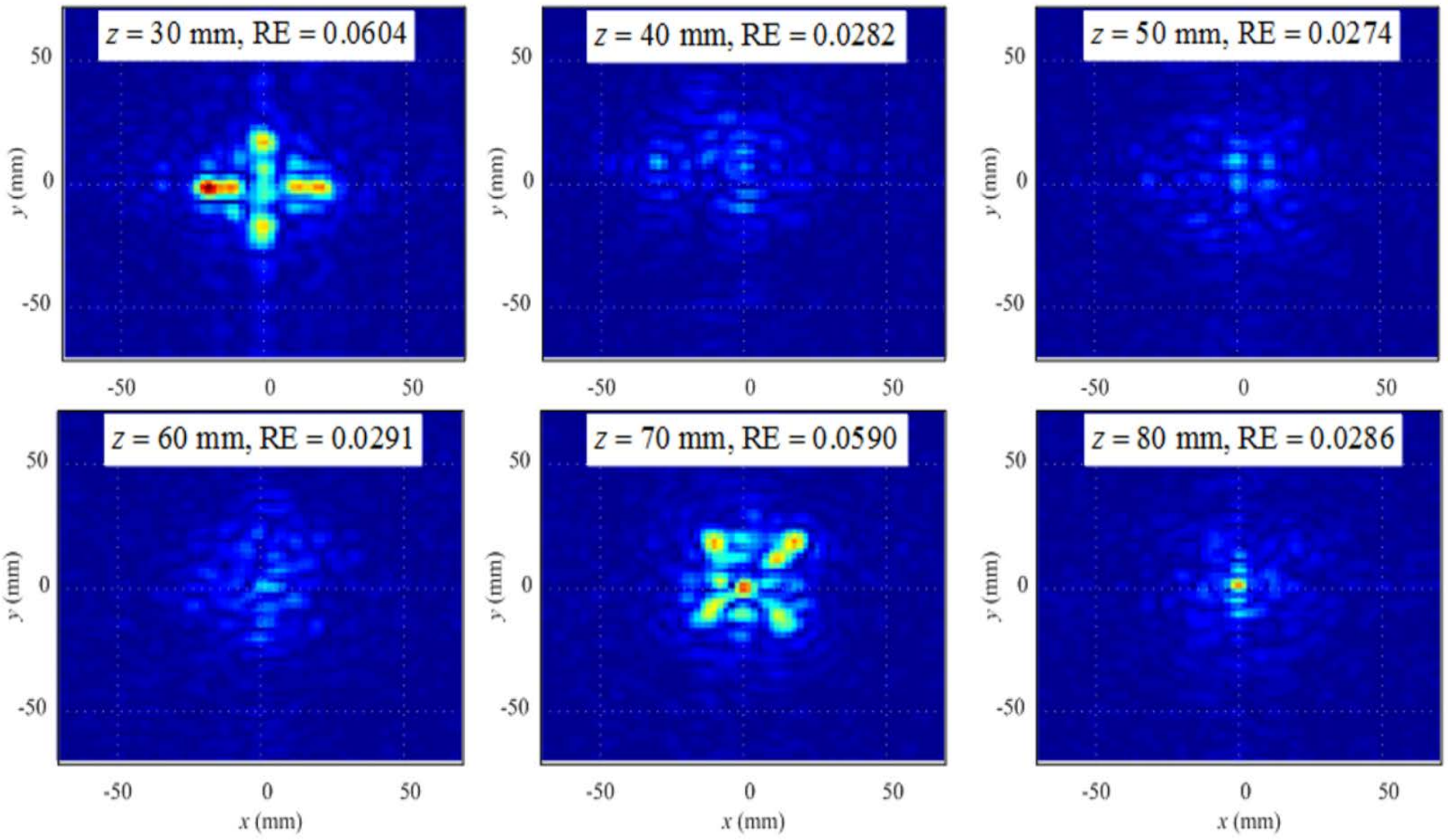

expected spatial resolution

depth:
$\delta_z \approx 10$ mm

lateral:
$\delta_{x,y} \approx 4$ mm

INVERSION WITH SCATTERED POWER MAPPING (SPM)

QUALITATIVE IMAGING WITH SENSITIVITY MAPS

- SPM is rooted in early work on the use of response sensitivities in image reconstruction
  [Y. Song, N.K. Nikolova, "Memory efficient method for wideband self-adjoint sensitivity analysis," *IEEE Trans. Microwave Theory Tech.*, 2008]
  [L. Liu, A. Trehan, N.K. Nikolova, "Near-field detection at microwave frequencies based on self-adjoint response sensitivity analysis," *Inv. Problems*, 2010]

- ***response sensitivities***: response derivatives with respect to some system parameters
- in imaging – ***derivatives with respect to permittivity*** at each voxel (Fréchet derivative)

- assume we want to minimize the ℓ_2-norm error between the measured OUT (total-field) and RO (incident-field) data

$$F[\varepsilon(\mathbf{r}')] = 0.5\sum_{\xi=1}^{N_T}\int_{\omega}\iint_{\mathbf{r}\in S_\mathrm{a}}\left\| S_\xi^{\mathrm{OUT}}(\mathbf{r},\omega) - S_\xi^{\mathrm{RO}}[\mathbf{r},\omega;\varepsilon(\mathbf{r}')]\right\|_2^2 d\mathbf{r}\,d\omega$$

- for that we need to know how to properly change the permittivity in the RO $\varepsilon_\mathrm{b}(\mathbf{r}') \xrightarrow{?} \varepsilon(\mathbf{r}')$
  - we need to know how the error function F would change when ε changes at $\forall \mathbf{r}'_n \in V_\mathrm{s}$

$$\boxed{\frac{\partial F}{\partial \varepsilon(\mathbf{r}'_n)} = ? \quad n = 1,\ldots,N_\mathrm{v}}$$

- Fréchet derivative with respect to $\varepsilon(\mathbf{r}') = \varepsilon'(\mathbf{r}') - \mathrm{i}\varepsilon''(\mathbf{r}')$

$$\operatorname{Re}\{D(\mathbf{r}')\} = \frac{\partial F}{\partial \varepsilon'(\mathbf{r}')}$$

→ indicates where contrast in ε' exists in the OUT

$$\operatorname{Im}\{D(\mathbf{r}')\} = -\frac{\partial F}{\partial \varepsilon''(\mathbf{r}')}$$

→ indicates where contrast in ε'' exists in the OUT

where

[Nikolova, *Introduction to Microwave Imaging*, 2017]

$$\underbrace{D(\mathbf{r}')}_{\text{sensitivity map}} = \sum_{\xi=1}^{N_T} \int_\omega \iint_{\mathbf{r}\in S_\mathrm{a}} \left[S_\xi^{\mathrm{RO}}(\mathbf{r},\omega) - S_\xi^{\mathrm{OUT}}(\mathbf{r},\omega) \right] \cdot \left[\frac{\partial S_\xi^{\mathrm{RO}}(\mathbf{r},\omega)}{\partial \varepsilon(\mathbf{r}')} \right]^* d\mathbf{r}\, d\omega$$

- ***sensitivity map***: 3-D plot of the real and imaginary parts of $D(\mathbf{r}')$

SENSITIVITY MAPS: FROM DERIVATIVES TO FINITE DIFFERENCES

$$D(\mathbf{r}') = \sum_{\xi=1}^{N_T} \int_\omega \iint_{\mathbf{r}\in S_\mathrm{a}} \underbrace{\left[S_\xi^{\mathrm{RO}}(\mathbf{r},\omega) - S_\xi^{\mathrm{OUT}}(\mathbf{r},\omega) \right]} \cdot \left[\frac{\partial S_\xi^{\mathrm{RO}}(\mathbf{r},\omega)}{\partial \varepsilon(\mathbf{r}')} \right]^* d\mathbf{r}\, d\omega$$

$-S_\xi^{\mathrm{sc}}(\mathbf{r},\omega)$ (Born approximation)

- approximating the response derivative with the PSF

$$\frac{\partial S_\xi^{\mathrm{RO}}(\mathbf{r},\omega)}{\partial \varepsilon(\mathbf{r}')} \approx \frac{\Delta S_\xi^{\mathrm{RO}}(\mathbf{r},\omega)}{\Delta \varepsilon(\mathbf{r}')} \approx \frac{S_\xi^{\mathrm{CO}}(\mathbf{r},\mathbf{r}';\omega) - S_\xi^{\mathrm{RO}}(\mathbf{r},\omega)}{\Delta \varepsilon_{\mathrm{sp}}(\mathbf{r}')} = \frac{S_\xi^{\mathrm{PSF}}(\mathbf{r},\mathbf{r}';\omega)}{\Delta \varepsilon_{\mathrm{sp}}}$$

position of scattering probe

$$\Rightarrow -\Delta\varepsilon_{\mathrm{sp}}^* \cdot D(\mathbf{r}') = \underbrace{M(\mathbf{r}')}_{\text{scattered power map}} = \sum_{\xi=1}^{N_T} \int_\omega \iint_{\mathbf{r}\in S_\mathrm{a}} S_\xi^{\mathrm{sc}}(\mathbf{r},\omega) \cdot \left[S_\xi^{\mathrm{PSF}}(\mathbf{r},\mathbf{r}';\omega) \right]^* d\mathbf{r}\, d\omega$$

SCATTERED-POWER MAPS: RECONSTRUCTION FORMULA

[Tu *et al.*, *Inv. Problems*, 2015][Shumakov *et al.*, *IEEE Trans. MTT*, 2018]

$$\underbrace{M(\mathbf{r}')}_{\text{scattered power map}} = \sum_{\xi=1}^{N_T} \int_{\omega} \iint_{\mathbf{r}\in S_{\mathrm{a}}} S_{\xi}^{\mathrm{sc}}(\mathbf{r},\omega) \cdot \left[S_{\xi}^{\mathrm{PSF}}(\mathbf{r},\mathbf{r}';\omega) \right]^* d\mathbf{r}\, d\omega$$

- ***scattered-power map***: 3-D qualitative image of the OUT contrast relative to the RO

SOME IMPORTANT ADVANTAGES

- reconstruction is practically instantaneous – no systems of equations are solved!

  … reconstruction formula is a simple summation of response products
- reconstruction can be carried out with ANY set of observation points (no need to have acquisition surfaces of canonical shapes (planar, cylindrical, spherical)

  … as long as the PSF is available analytically or from measurements

SCATTERED-POWER MAPS AND TEMPORAL CROSS-CORRELATION

- SPM image $M(\mathbf{r}')$ can be viewed as a plot of the ***aggregate measure of similarity*** between the OUT responses and the respective PSF responses due to point scatterer at $\mathbf{r}'$

$$M(\mathbf{r}') = \sum_{\xi=1}^{N_T} \int_{\omega} \iint_{\mathbf{r}\in S_\mathrm{a}} S_\xi^{\mathrm{sc}}(\mathbf{r},\omega)\cdot\left[S_\xi^{\mathrm{PSF}}(\mathbf{r},\mathbf{r}';\omega)\right]^* d\mathbf{r}\, d\omega = \sum_{\xi=1}^{N_T} \int_{\omega} \iint_{\mathbf{r}\in S_\mathrm{a}} \mathcal{F}_t \underbrace{\left\{S_\xi^{\mathrm{sc}}(\mathbf{r},t)\otimes S_\xi^{\mathrm{PSF}}(\mathbf{r},\mathbf{r}';t)\right\}}_{\text{cross-correlation } X_\xi(\mathbf{r},\mathbf{r}';\tau)} d\mathbf{r}\, d\omega$$

- reminder: cross-correlation is a measure of similarity between 2 waveforms as a function of their mutual time-shift

- it can be shown that (with infinite bandwidth)

no shift

$$\boxed{M(\mathbf{r}') \sim \sum_{\xi=1}^{N_T} \iint_{\mathbf{r}\in S_\mathrm{a}} X_\xi(\mathbf{r},\mathbf{r}';\tau=0)\, d\mathbf{r}}$$

SCATTERED-POWER MAPS AND CROSS-CORRELATION IN SPACE

- consider planar scanning and assume lateral translational invariance of the PSF

$$S_\xi^{\text{PSF}}(x, y, \bar{z}; x', y', z'; \omega) \approx S_{\xi 0}^{\text{PSF}}\left(x - x', y - y', \bar{z}; z'; \omega\right)$$

$$\Rightarrow \quad M(x', y', z') = \sum_{\xi=1}^{N_T} \int_\omega \underbrace{\iint_{S_\text{a}} S_\xi^{\text{sc}}(x, y, \bar{z}, \omega) \cdot \left[S_{\xi 0}^{\text{PSF}}\left(x - x', y - y', \bar{z}; z'; \omega\right)\right]^* dxdy}_{\text{cross-correlation in } (x,y)} \, d\omega$$

- image reconstruction formula

$$\Rightarrow \quad M(x', y', z') = \mathcal{F}_{\text{2D}}^{-1}\left\{ \sum_{\xi=1}^{N_T} \sum_{m=1}^{N_\omega} \tilde{S}_\xi^{\text{sc}}(k_x, k_y, \bar{z}, \omega) \cdot \left[\tilde{S}_{\xi 0}^{\text{PSF}}\left(k_x, k_y, \bar{z}; z'; \omega\right)\right]^* \right\}$$

SIMULATION EXAMPLE: QUALITATIVE SPM IMAGE OF F-SHAPE

simulation of PSF acquisition

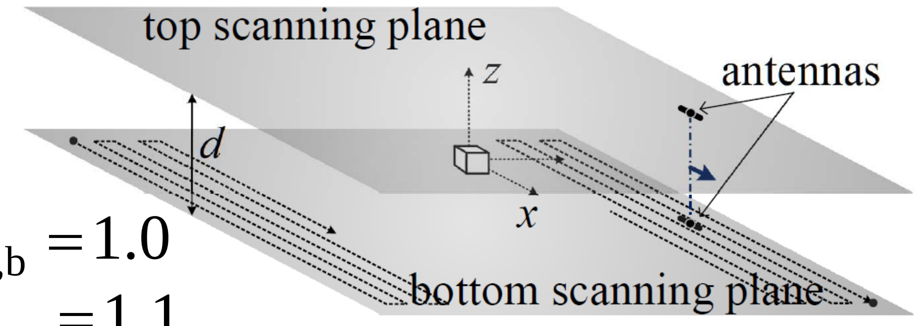

$\varepsilon_{\mathrm{r,b}} = 1.0$

$\varepsilon_{\mathrm{r,sp}} = 1.1$

simulation of data acquisition

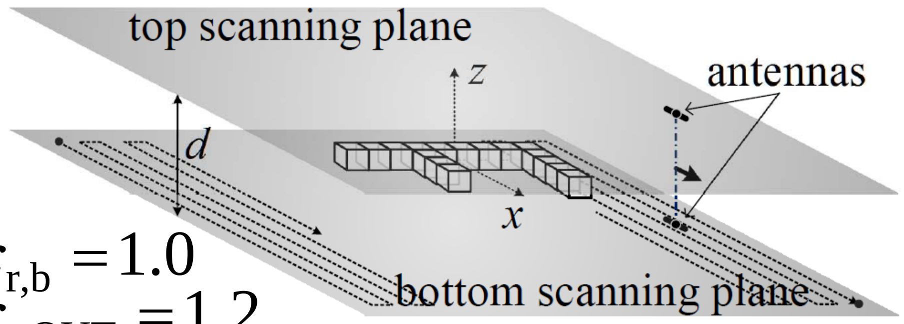

$\varepsilon_{\mathrm{r,b}} = 1.0$

$\varepsilon_{\mathrm{r,OUT}} = 1.2$

Altair FEKO

sample PSF: S_{11} at 4 GHz MAG/PHASE

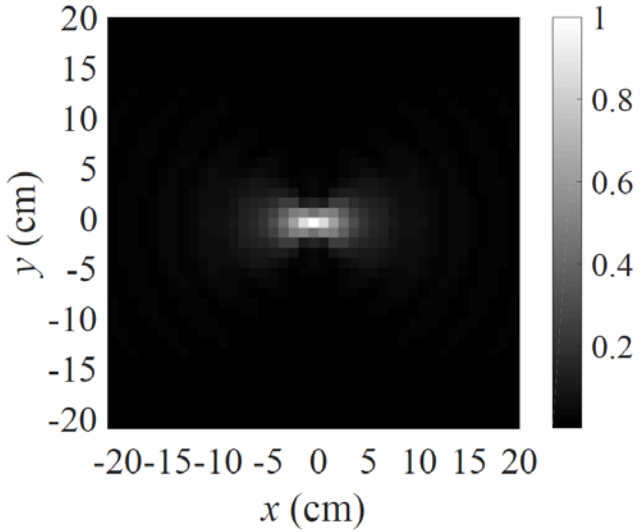

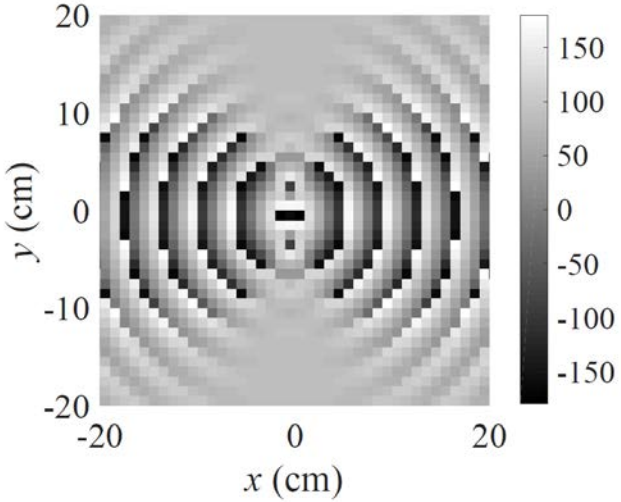

$f_{\min} = 3$ GHz

$f_{\max} = 16$ GHz

$\Delta f = 1$ GHz

SIMULATION EXAMPLE: QUALITATIVE SPM IMAGE OF F-SHAPE – 2

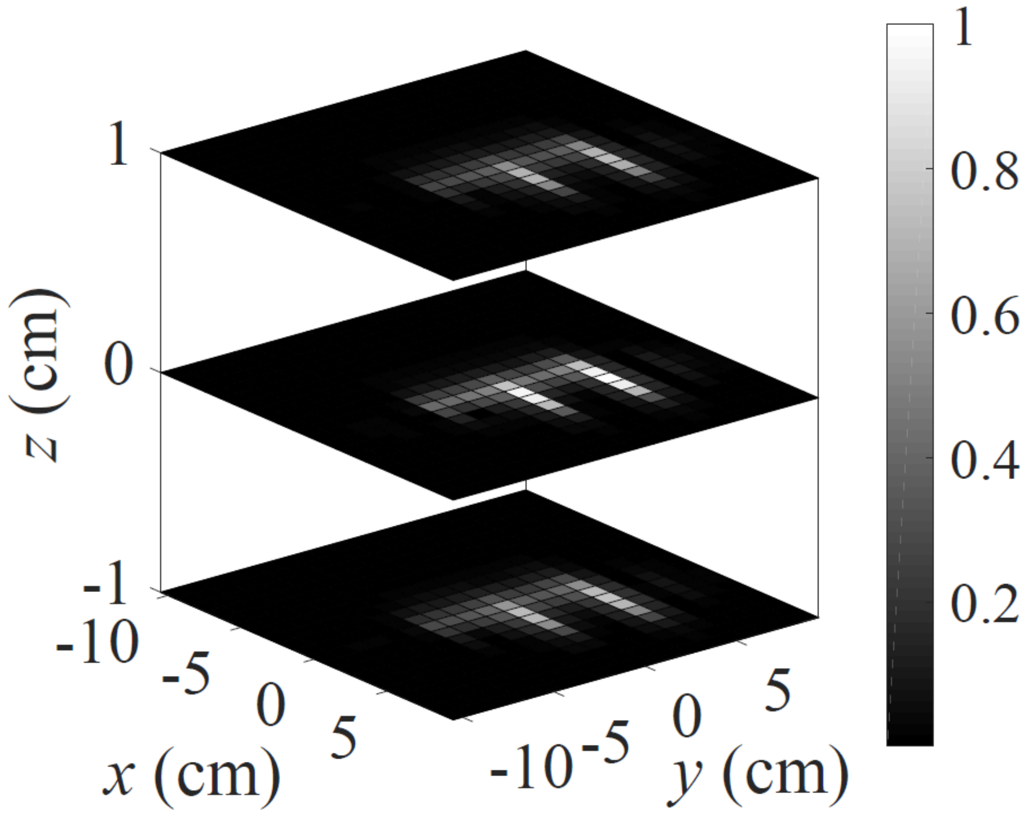

- blurring typical for cross-correlation methods
  - ➢ limited number of responses
  - ➢ diffraction limit on resolution

QUANTITATIVE SPM WITH MEASURED PSFs

- quantitative SPM uses the qualitative maps to improve the image quality significantly

$$M(x', y', z') = \sum_{\xi=1}^{N_T} \int_{\omega} \iint_{S_a} S_{\xi}^{\text{sc}}(x, y, \bar{z}, \omega) \cdot \left[S_{\xi 0}^{\text{PSF}}(x - x', y - y', \bar{z}; z'; \omega) \right]^* dxdy\, d\omega$$

$$S_{\xi}^{\text{sc}}(x, y, \bar{z}; \omega) \approx \frac{1}{\Delta\varepsilon_{\text{r,sp}} \Delta\Omega_{\text{sp}}} \int_{x'} \int_{y'} \int_{z'} \Delta\varepsilon_{\text{r}}(x', y', z') S_{\xi 0}^{\text{PSF}}(x - x', y - y', \bar{z}; z'; \omega)\, dx'dy'dz', \; \xi = 1, \ldots, N_T$$

$$\Rightarrow \quad \boxed{M(x', y', z') = \frac{1}{\Delta\varepsilon_{\text{r,sp}} \Omega_{\text{sp}}} \iiint_{V_s} \Delta\varepsilon_{\text{r}}(x'', y'', z'') \cdot M_{\text{sp}@(x'', y'', z'')}(x', y', z') dx''dy''dz''}$$

qualitative SPM image of OUT

unknown contrast

qualitative SPM image of scattering probe when it is at (x'', y'', z'')

QUANTITATIVE SPM: SOLUTION IN FOURIER SPACE

- quantitative SPM solves the linear problem

$$M(x',y',z') = \frac{1}{\Delta\varepsilon_{\mathrm{r,sp}}\Omega_{\mathrm{sp}}} \iiint_{V_{\mathrm{s}}} \Delta\varepsilon_{\mathrm{r}}(x'',y'',z'') \cdot M_{\mathrm{sp}@(x'',y'',z'')}(x',y',z')dx''dy''dz''$$

- linear system of equations can be quite large in real space: square system of size $N_{\mathrm{v}} \times N_{\mathrm{v}}$
- solving in Fourier (*k*-) space is much faster (similar to holography)
- assumption of medium ***lateral uniformity***: a shift in the position of the scattering probe leads to a corresponding shift in its qualitative map obtained with the central PSF

$$M_{\mathrm{sp}@(x'',y'',z'')}(x',y',z') = M_{\mathrm{sp}@(0,0,z'')}(x'-x'',y'-y'',z')$$

$$\Rightarrow M(x',y',z') = \frac{1}{\Delta\varepsilon_{\mathrm{r,sp}}\Omega_{\mathrm{sp}}} \int_{z''} \underbrace{\int_{y''}\int_{x''} \Delta\varepsilon_{\mathrm{r}}(x'',y'',z'') \cdot M_{\mathrm{sp}@(0,0,z'')}(x'-x'',y'-y'',z')\,dx''dy''}_{\text{convolution in } (x,y)}\,dz''$$

QUANTITATIVE SPM: SOLUTION IN FOURIER SPACE – 2

$$\tilde{M}(k_x,k_y,z_p)=\frac{\Omega_{\mathrm{v}}}{\Delta\varepsilon_{\mathrm{r,sp}}\Omega_{\mathrm{sp}}}\sum_{q=1}^{N_z}\tilde{f}(k_x,k_y,z_q)\cdot\tilde{M}_{\mathrm{sp}@(0,0,z_q)}(k_x,k_y,z_p),\ \ p=1,\ldots,N_z$$

- small square system of equations is solved ***at each spectral position*** $\boldsymbol{\kappa}=(k_x,k_y)$

$$\boxed{\boldsymbol{M}_{(\boldsymbol{\kappa})}\boldsymbol{x}_{(\boldsymbol{\kappa})}=\boldsymbol{m}_{(\boldsymbol{\kappa})}}$$

$$\boldsymbol{x}_{(\boldsymbol{\kappa})}=\left[\,\tilde{f}(\boldsymbol{\kappa},z_1)\cdots\tilde{f}(\boldsymbol{\kappa},z_{N_z})\right]^T$$

$$\boldsymbol{m}_{(\boldsymbol{\kappa})}=\left[\,\tilde{M}(\boldsymbol{\kappa},z_1)\cdots\tilde{M}(\boldsymbol{\kappa},z_{N_z})\right]^T$$

$$\boldsymbol{M}_{(\boldsymbol{\kappa})}=\begin{bmatrix}\tilde{M}_{\mathrm{sp}@(0,0,z_1)}(\boldsymbol{\kappa},z_1) & \cdots & \tilde{M}_{\mathrm{sp}@(0,0,z_{N_z})}(\boldsymbol{\kappa},z_1)\\ \vdots & \ddots & \vdots\\ \tilde{M}_{\mathrm{sp}@(0,0,z_1)}(\boldsymbol{\kappa},z_{N_z}) & \cdots & \tilde{M}_{\mathrm{sp}@(0,0,z_{N_z})}(\boldsymbol{\kappa},z_{N_z})\end{bmatrix}$$

- final step: back to (x,y) space

$$\Delta\varepsilon_r(x',y',z'_n)=\frac{\Delta\varepsilon_{\mathrm{r,sp}}\Omega_{\mathrm{sp}}}{\Omega_{\mathrm{v}}}\mathcal{F}_{\mathrm{2D}}^{-1}\left\{\tilde{f}(\boldsymbol{\kappa};z'_n)\right\},\ n=1,\ldots,N_z$$

SIMULATION EXAMPLE: QUANTITATIVE SPM IMAGE OF F-SHAPE

[Shumakov, in Nikolova, *Introduction to Microwave Imaging*, 2017]

$\mathrm{Re}\,\varepsilon_{\mathbf{r}}$

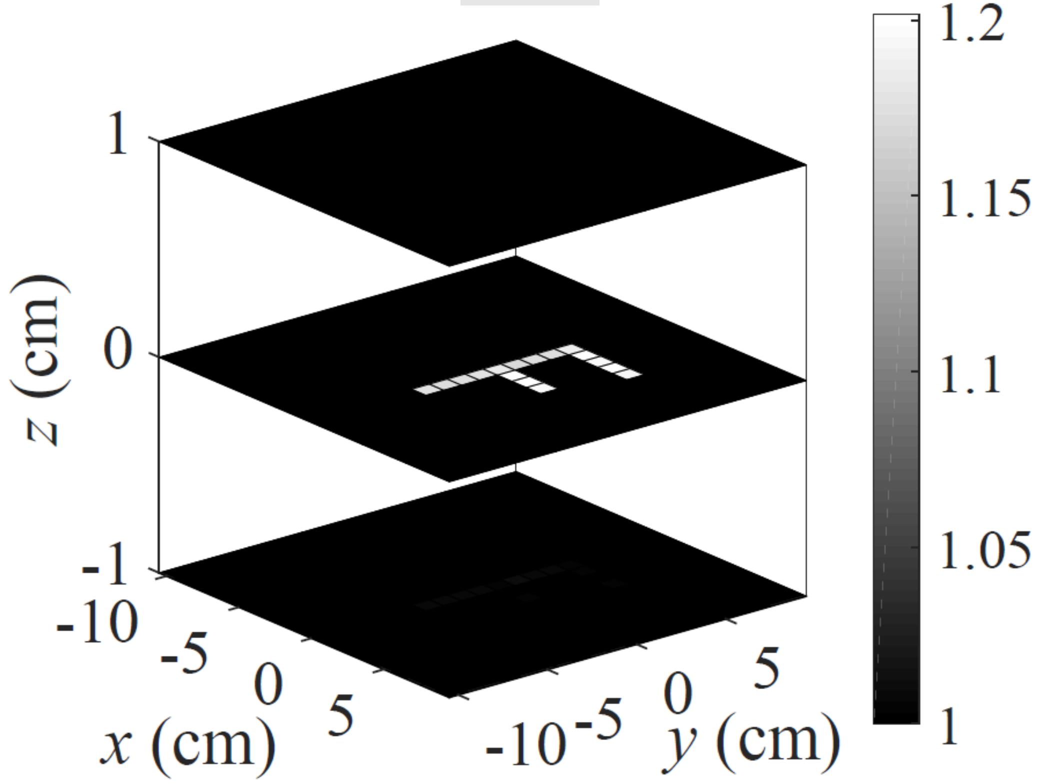

$\mathrm{Im}\,\varepsilon_{\mathbf{r}}$

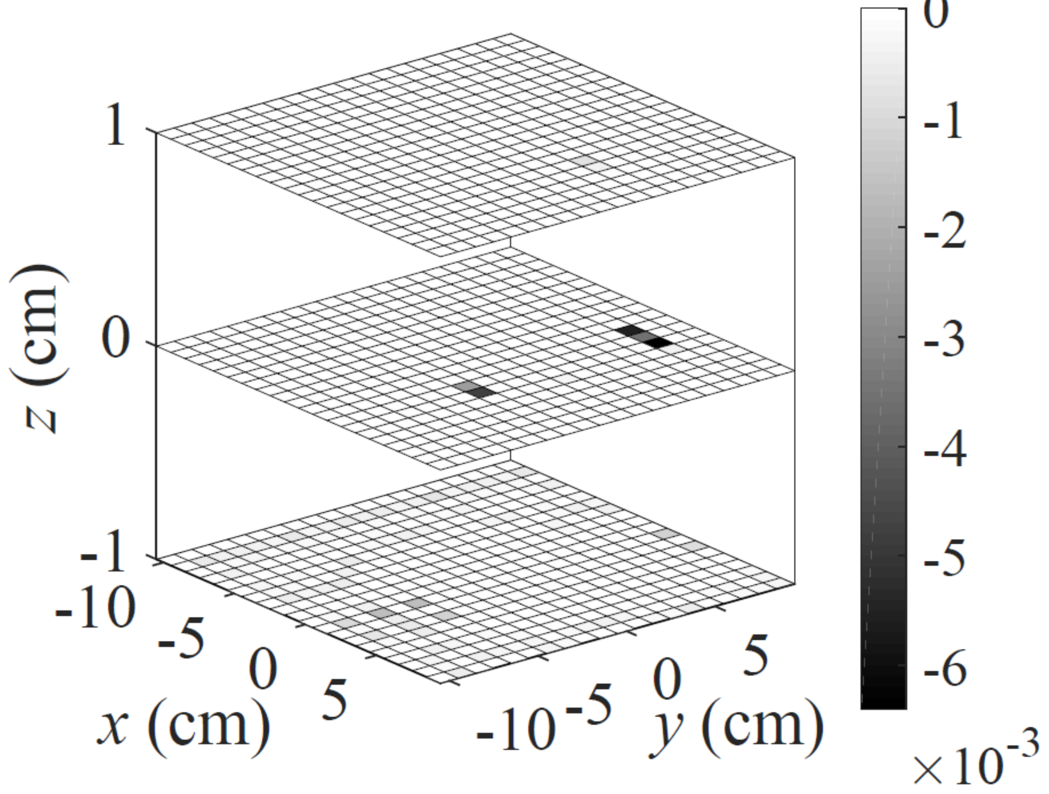

EXPERIMENTAL EXAMPLE: QUANTITATIVE SPM

[Shumakov *et al.*, *IEEE Trans. MTT*, 2018]

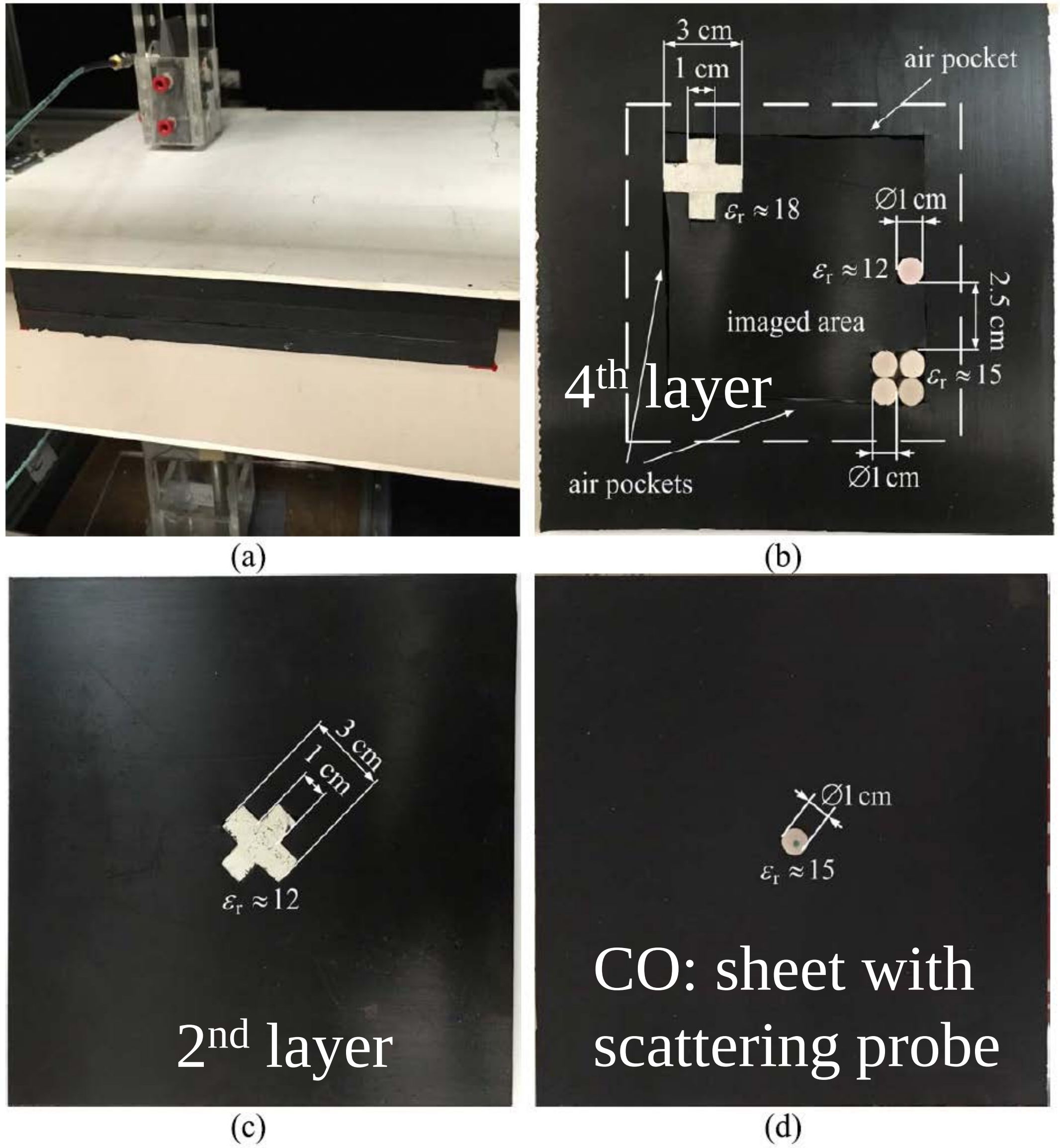

- 5 cm thick carbon-rubber sample $\varepsilon_{r,b} \approx 10 - i5$
- frequency: from 3 GHz to 9 GHz (61 samples) $\varepsilon_{r,sp} \approx 15 - i0.003$
- scattering probe
- all embedded objects are 1 cm thick
- reflection and transmission coefficients on two TEM horn antennas aligned along boresight
- imaged area 13 cm by 13 cm (2 mm sampling step)

EXPERIMENTAL EXAMPLE: QUANTITATIVE SPM – IMAGES

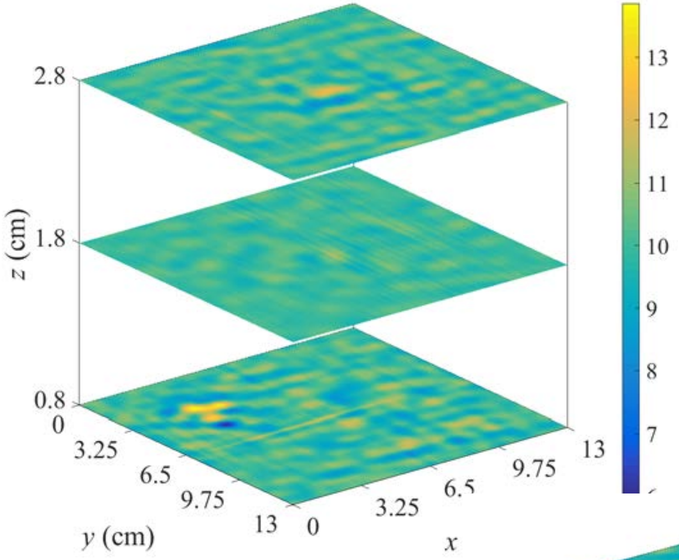

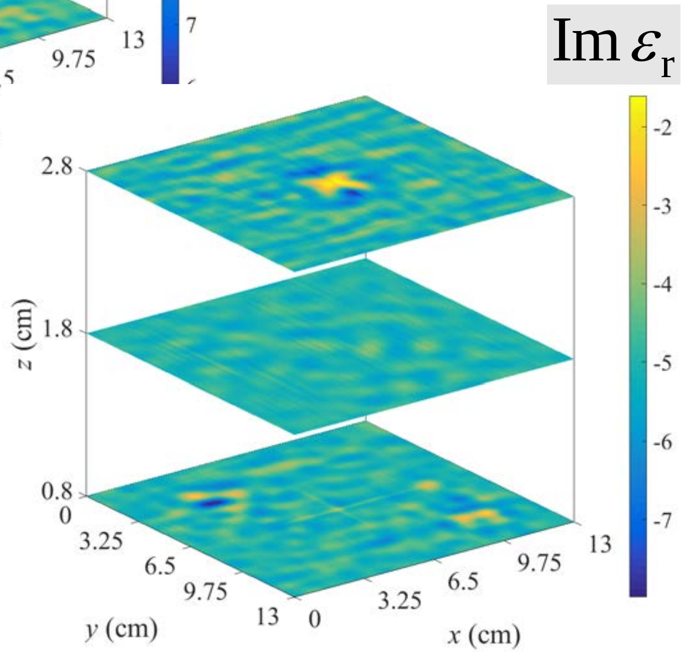

Born approximation

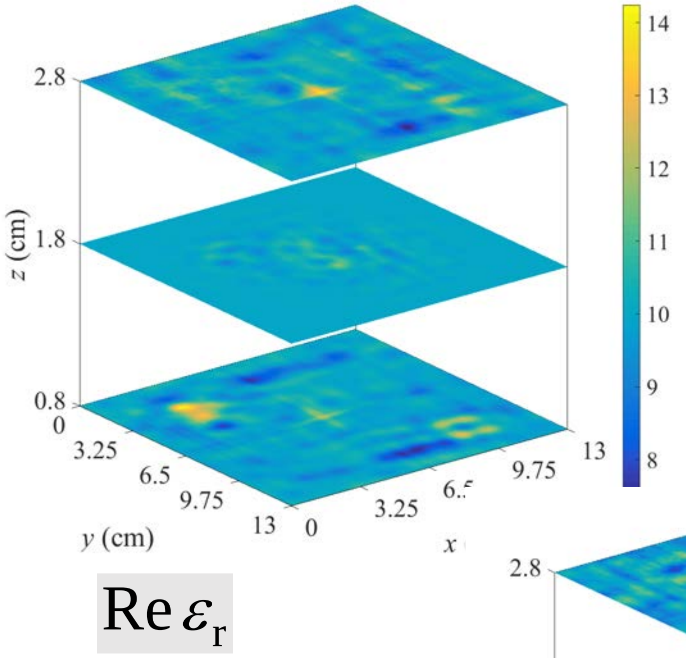

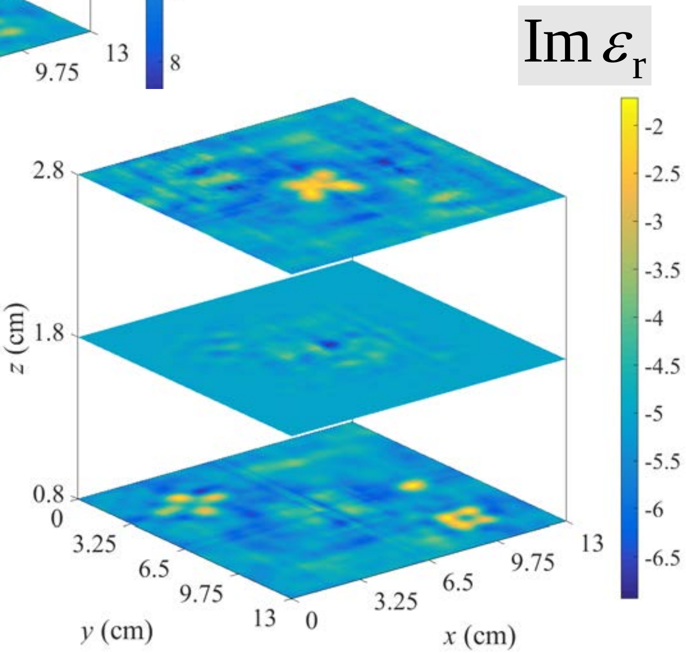

Rytov approximation

[Shumakov *et al.*, *IEEE Trans. MTT*, 2018]

EXPERIMENTAL EXAMPLE: TEDDY BEAR 2-D IMAGE

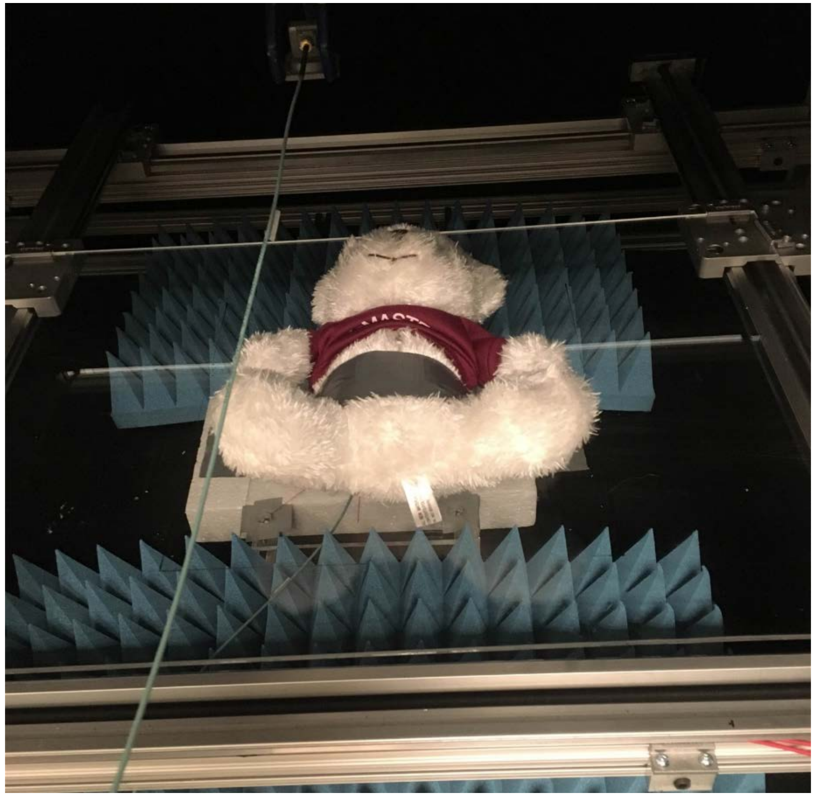

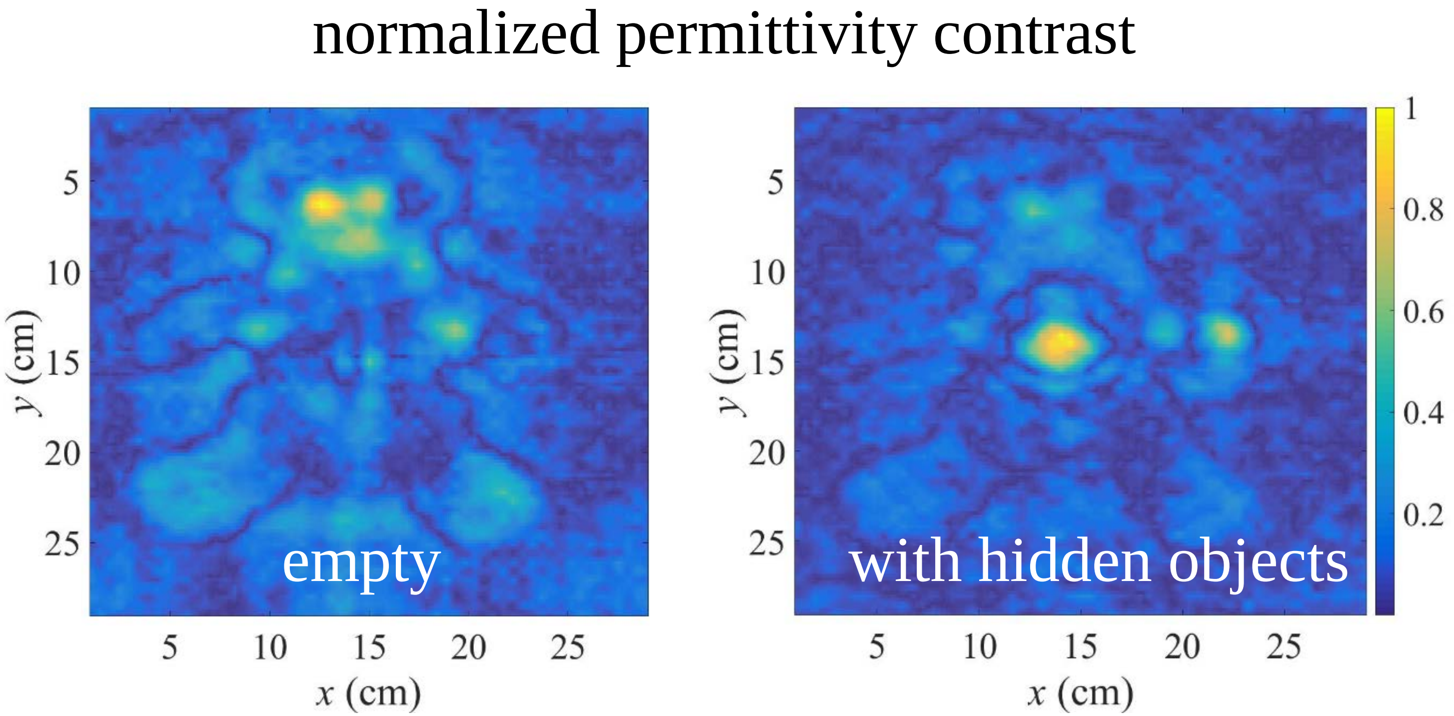

INVERSION WITH SYNTHETIC FOCUSING

SYNTHETIC FOCUSING: MATCHED FILTERING

- synthetic focusing is the process of cross-correlating each measured signal with a signal, which represents the radar response to a point scatterer at $\mathbf{r}'$ (this is just the system PSF)

signal recorded at $\mathbf{r}$ *"focused" on* $\mathbf{r}'$ ⟶

$$\boxed{x_\xi(\mathbf{r},\mathbf{r}';t) = S_\xi^{\mathrm{sc}}(\mathbf{r},t) \otimes S_\xi^{\mathrm{PSF}}(\mathbf{r},\mathbf{r}';t)}$$

- this computation is known as ***matched filtering*** – it checks how well a signal "matches" the PSF at $\mathbf{r}'$ for all time shifts

- Why is this called "filtering"?

in the frequency domain: $X(\mathbf{r}';\omega) = \sum_{\xi=1}^{N_T} \iint_{\mathbf{r}\in S_a} \overbrace{S_\xi^{\mathrm{sc}}(\mathbf{r},\omega) \cdot \underbrace{\left[S_\xi^{\mathrm{PSF}}(\mathbf{r},\mathbf{r}';\omega)\right]^*}_{H_\xi(\mathbf{r},\mathbf{r}';\omega)}}^{X_\xi(\mathbf{r},\mathbf{r}';\omega)} d\mathbf{r}$

$$\underbrace{S_\xi^{\mathrm{sc}}(\mathbf{r},\omega)}_{\text{input}} \cdot \underbrace{H_\xi(\mathbf{r},\mathbf{r}';\omega)}_{\text{filter}} = \underbrace{X_\xi(\mathbf{r},\mathbf{r}';\omega)}_{\text{output}}$$

↑ *transfer function of the matched filter (aka **steering filter**)*

SYNTHETIC FOCUSING: SIGNAL PROCESSING STAGES

- STAGE 1: matched filtering of all measured responses with "focus" on $\mathbf{r}'$

$$x_\xi(\mathbf{r},\mathbf{r}';t) = \underbrace{S_\xi^{\mathrm{sc}}(\mathbf{r},t) \otimes S_\xi^{\mathrm{PSF}}(\mathbf{r},\mathbf{r}';t)}_{\text{cross-correlation}} = \underbrace{S_\xi^{\mathrm{sc}}(\mathbf{r},t) * h_\xi(\mathbf{r},\mathbf{r}';t)}_{\text{convolution}}$$

matched filter impulse response

- STAGE 2: summing up all $\mathbf{r}'$-focused responses at each time instant

$$y(\mathbf{r}';t_n) = \sum_{\xi=1}^{N_T} \underbrace{\iint_{\mathbf{r}\in S_\mathrm{a}} x_\xi(\mathbf{r},\mathbf{r}';t_n)\,d\mathbf{r}}_{\text{integrating over radar aperture}} = \sum_{\xi=1}^{N_T} \iint_{\mathbf{r}\in S_\mathrm{a}} \left[S_\xi^{\mathrm{sc}}(\mathbf{r},t) \otimes S_\xi^{\mathrm{PSF}}(\mathbf{r},\mathbf{r}';t) \right]_{(t_n)} d\mathbf{r}\,, \quad n = 0,1,\ldots,N_t$$

- STAGE 3: windowing focused output to suppress radar clutter

$$y_w(\mathbf{r}';t_n) = y(\mathbf{r}';t_n)\cdot w(t_n),\ n = 0,1,\ldots,N_t$$

- STAGE 4: calculating scattering intensity at $\mathbf{r}'$

$$I(\mathbf{r}') = \int_t y_w^2(\mathbf{r}',t)\,dt \quad \Rightarrow \quad \boxed{\text{PLOT as function of } \mathbf{r}'}$$

SYNTHETIC FOCUSING: SIGNAL-FLOW SCHEMATIC

[Nikolova, *Introduction to Microwave Imaging*, 2017]

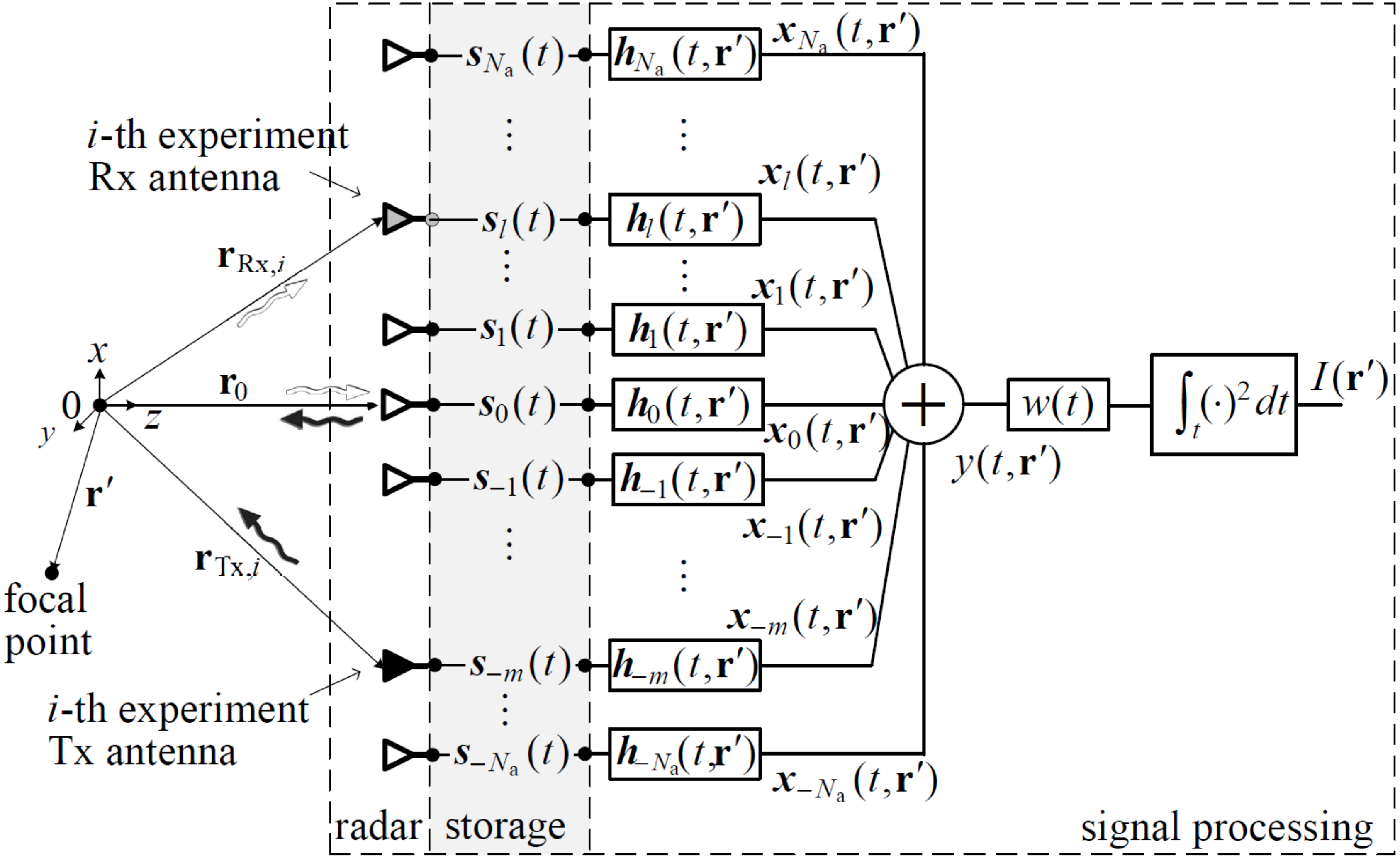

- core computation in synthetic focusing

$$y(\mathbf{r}';t) = \sum_{\xi=1}^{N_T} \iint_{\mathbf{r}\in S_\mathrm{a}} \left[S_\xi^{\mathrm{sc}}(\mathbf{r}) \otimes S_\xi^{\mathrm{PSF}}(\mathbf{r},\mathbf{r}') \right]_{(t)} d\mathbf{r}$$

- time-domain linear model of scattering (inverse FT of the frequency-domain model)

$$S_\xi^{\mathrm{sc}}(\mathbf{r};\omega) \sim \iiint_{V_\mathrm{s}} \Delta\varepsilon_\mathrm{r}(\mathbf{r}') \cdot S_\xi^{\mathrm{PSF}}(\mathbf{r};\mathbf{r}';\omega)\, d\mathbf{r}' \Rightarrow S_\xi^{\mathrm{sc}}(\mathbf{r};t) \sim \iiint_{V_\mathrm{s}} \Delta\varepsilon_\mathrm{r}(\mathbf{r}') \cdot S_\xi^{\mathrm{PSF}}(\mathbf{r};\mathbf{r}';t) d\mathbf{r}'$$

$$\Rightarrow \quad y(\mathbf{r}';t) \sim \iiint_{\mathbf{r}''\in V_\mathrm{s}} \Delta\varepsilon_\mathrm{r}(\mathbf{r}'') \cdot \sum_{\xi=1}^{N_T} \iint_{\mathbf{r}\in S_\mathrm{a}} \left[S_\xi^{\mathrm{PSF}}(\mathbf{r},\mathbf{r}') \otimes S_\xi^{\mathrm{PSF}}(\mathbf{r},\mathbf{r}'') \right]_{(t)} d\mathbf{r}\, d\mathbf{r}''$$

UNDERSTANDING SYNTHETIC FOCUSING – 2

$$y(\mathbf{r}';t) \sim \iiint_{\mathbf{r}''\in V_\mathrm{s}} \Delta\varepsilon_\mathrm{r}(\mathbf{r}'') \cdot \sum_{\xi=1}^{N_T} \iint_{\mathbf{r}\in S_\mathrm{a}} \left[S_\xi^{\mathrm{PSF}}(\mathbf{r},\mathbf{r}') \otimes S_\xi^{\mathrm{PSF}}(\mathbf{r},\mathbf{r}'') \right]_{(t)} d\mathbf{r}\, d\mathbf{r}''$$

- with large number of responses, the strength of $y(\mathbf{r}';t)$ is proportional to the contrast $\Delta\varepsilon_\mathrm{r}(\mathbf{r}')$ because the autocorrelation term dominates the integral over $\mathbf{r}''$
  - autocorrelation term: $\mathbf{r}'' = \mathbf{r}' \;\Rightarrow \Delta\varepsilon_\mathrm{r}(\mathbf{r}') \cdot \sum_{\xi=1}^{N_T} \iint_{\mathbf{r}\in S_\mathrm{a}} \left[S_\xi^{\mathrm{PSF}}(\mathbf{r},\mathbf{r}') \otimes S_\xi^{\mathrm{PSF}}(\mathbf{r},\mathbf{r}') \right]_{(t)} d\mathbf{r}$
  - cross-correlation terms: $\mathbf{r}'' \neq \mathbf{r}' \Rightarrow \;\Delta\varepsilon_\mathrm{r}(\mathbf{r}'') \cdot \sum_{\xi=1}^{N_T} \iint_{\mathbf{r}\in S_\mathrm{a}} \left[S_\xi^{\mathrm{PSF}}(\mathbf{r},\mathbf{r}') \otimes S_\xi^{\mathrm{PSF}}(\mathbf{r},\mathbf{r}'') \right]_{(t)} d\mathbf{r}$

    integration over incoherent weak x-correlations

DELAY AND SUM (DAS) RECONSTRUCTION ALGORITHM

- DAS is the simplest synthetic-focusing algorithm
- it assumes a PSF of the form (same for all response types and antennas)

$$S^{\mathrm{PSF}}(\mathbf{r}_{\mathrm{Rx}},\mathbf{r}_{\mathrm{Tx}};\mathbf{r}';t) \sim \delta\left(t + t_0 - \frac{r_{\mathrm{Tx}}(\mathbf{r}') + r_{\mathrm{Rx}}(\mathbf{r}')}{v_{\mathrm{b}}}\right) / \boxed{(r_{\mathrm{Tx}} r_{\mathrm{Rx}})}, \text{ where } r_{\mathrm{Tx}} = |\mathbf{r}' - \mathbf{r}_{\mathrm{Tx}}|,\ r_{\mathrm{Rx}} = |\mathbf{r}' - \mathbf{r}_{\mathrm{Rx}}|$$

reference time for scattering center at origin

often ignored with far-zone measurements

- for a point scatterer at the reference point (origin)

$$S^{\mathrm{PSF}}(\mathbf{r}_{\mathrm{Rx}},\mathbf{r}_{\mathrm{Tx}};\mathbf{r}'=0;t) \equiv S_0^{\mathrm{PSF}}(\mathbf{r}_{\mathrm{Rx}},\mathbf{r}_{\mathrm{Tx}};t)$$
$$\sim \delta\left(t + t_0 - \frac{|\mathbf{r}_{\mathrm{Tx}}| + |\mathbf{r}_{\mathrm{Rx}}|}{v_{\mathrm{b}}}\right)$$

  - ➢ origin often chosen at furthest point and

$$t_0 = \frac{|\mathbf{r}_{\mathrm{Tx}}| + |\mathbf{r}_{\mathrm{Rx}}|}{v_{\mathrm{b}}} \quad \text{so that} \quad S_0^{\mathrm{PSF}}(\mathbf{r}_{\mathrm{Rx}},\mathbf{r}_{\mathrm{Tx}};t) = \delta(t)$$

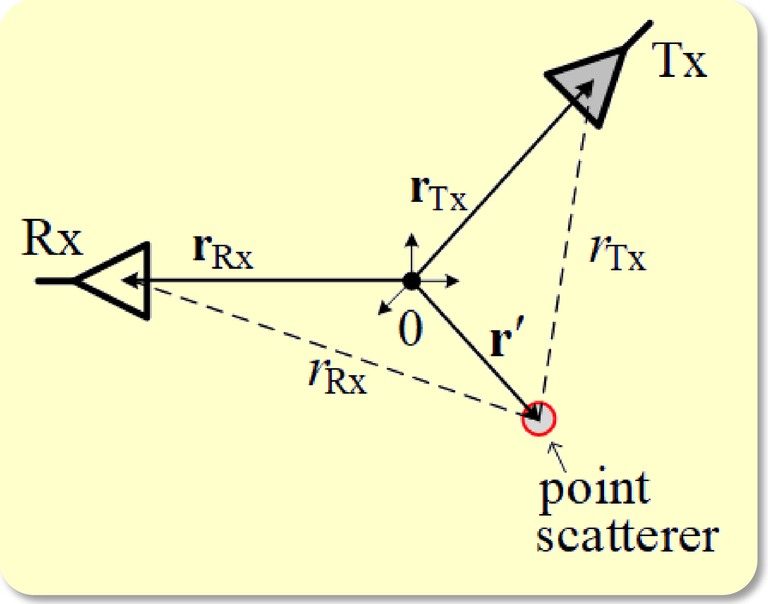

DELAY AND SUM (DAS) RECONSTRUCTION ALGORITHM – 2

- DAS PSF is a plane wave in the frequency domain

$$\boxed{S^{\mathrm{PSF}}(\mathbf{r}_{\mathrm{Rx}},\mathbf{r}_{\mathrm{Tx}};\mathbf{r}';\omega)=e^{-\mathrm{i}k_{\mathrm{b}}(r_{\mathrm{Tx}}+r_{\mathrm{Rx}}-r_0)}} \longleftrightarrow \delta\left(t+t_0-\frac{r_{\mathrm{Tx}}(\mathbf{r}')+r_{\mathrm{Rx}}(\mathbf{r}')}{v_{\mathrm{b}}}\right)$$

where

$k_{\mathrm{b}}=\omega/v_{\mathrm{b}}$ (wavenumber)

$r_0=|\mathbf{r}_{\mathrm{Tx}}|+|\mathbf{r}_{\mathrm{Rx}}|=v_{\mathrm{b}}t_0$ (signal path through reference point)

- DAS matched filters

$$H(\mathbf{r}_{\mathrm{Rx}},\mathbf{r}_{\mathrm{Tx}};\mathbf{r}';\omega)=(S^{\mathrm{PSF}})^*=e^{\mathrm{i}k_{\mathrm{b}}(r_{\mathrm{Tx}}+r_{\mathrm{Rx}}-r_0)} \Rightarrow h(\mathbf{r}_{\mathrm{Rx}},\mathbf{r}_{\mathrm{Tx}};\mathbf{r}';t)=\delta\left(t-t_0+\frac{r_{\mathrm{Tx}}+r_{\mathrm{Rx}}}{v_{\mathrm{b}}}\right)$$

DELAY AND SUM (DAS) RECONSTRUCTION ALGORITHM – 3

- DAS synthetic focusing

matched filter

$$y(\mathbf{r}';t) = \sum_{\xi=1}^{N_T} \iint_{\mathbf{r}\in S_a} S_{\xi}^{sc}(\mathbf{r};t) * \delta\left(t - t_0 + \frac{r_{Tx} + r_{Rx}}{v_b}\right) d\mathbf{r}$$

$$= \sum_{\xi=1}^{N_T} \iint_{\mathbf{r}\in S_a} \int_{\tau} S_{\xi}^{sc}(\mathbf{r};\tau)\delta\left(t - t_0 + \frac{r_{Tx} + r_{Rx}}{v_b} - \tau\right) d\tau\, d\mathbf{r} \longleftarrow \textit{sifting property of } \delta\textit{-function}$$

$$= \underbrace{\sum_{\xi=1}^{N_T} \iint_{\mathbf{r}\in S_a} \underbrace{S_{\xi}^{sc}\left(\mathbf{r};t - \left(t_0 - \frac{r_{Tx} + r_{Rx}}{v_b}\right)\right)}_{\text{response is "delayed"}} d\mathbf{r}}_{\text{responses colected over aperture are "delayed and sumed"}}$$

- DAS focusing is nothing but a time-shift of the response so as to virtually space-shift the scattering center from $\mathbf{r}'$ to the origin (reference point)

DAS: CONCEPTUAL EXAMPLE

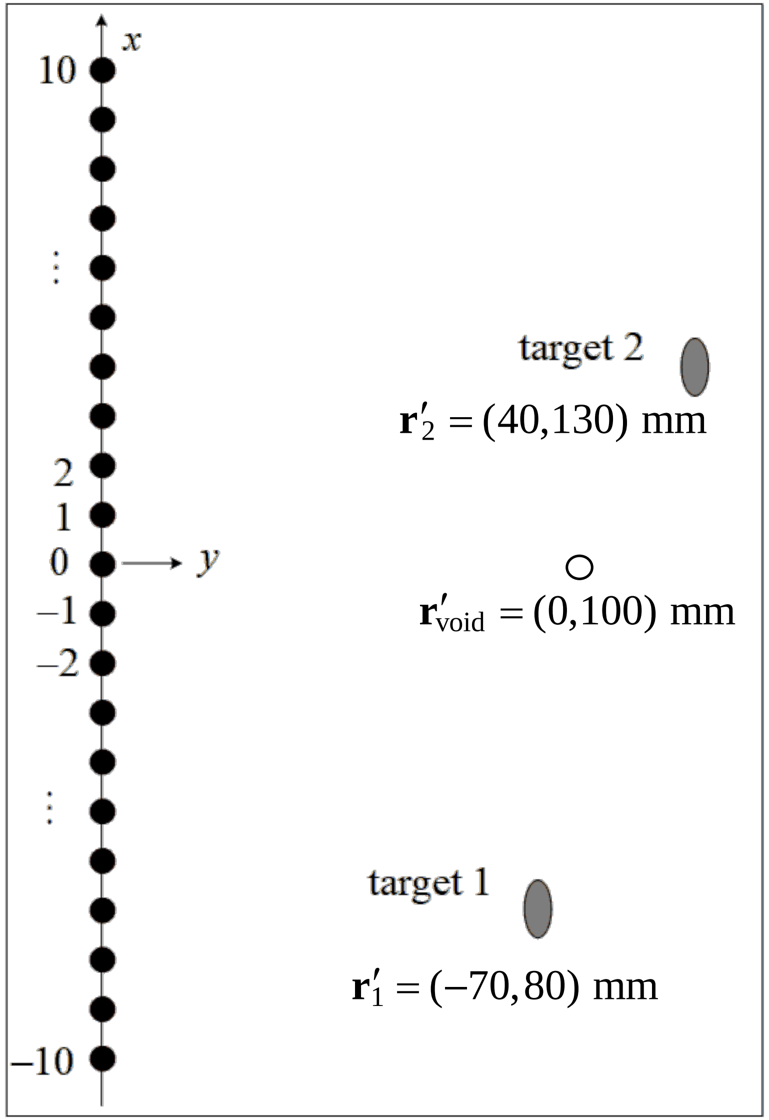

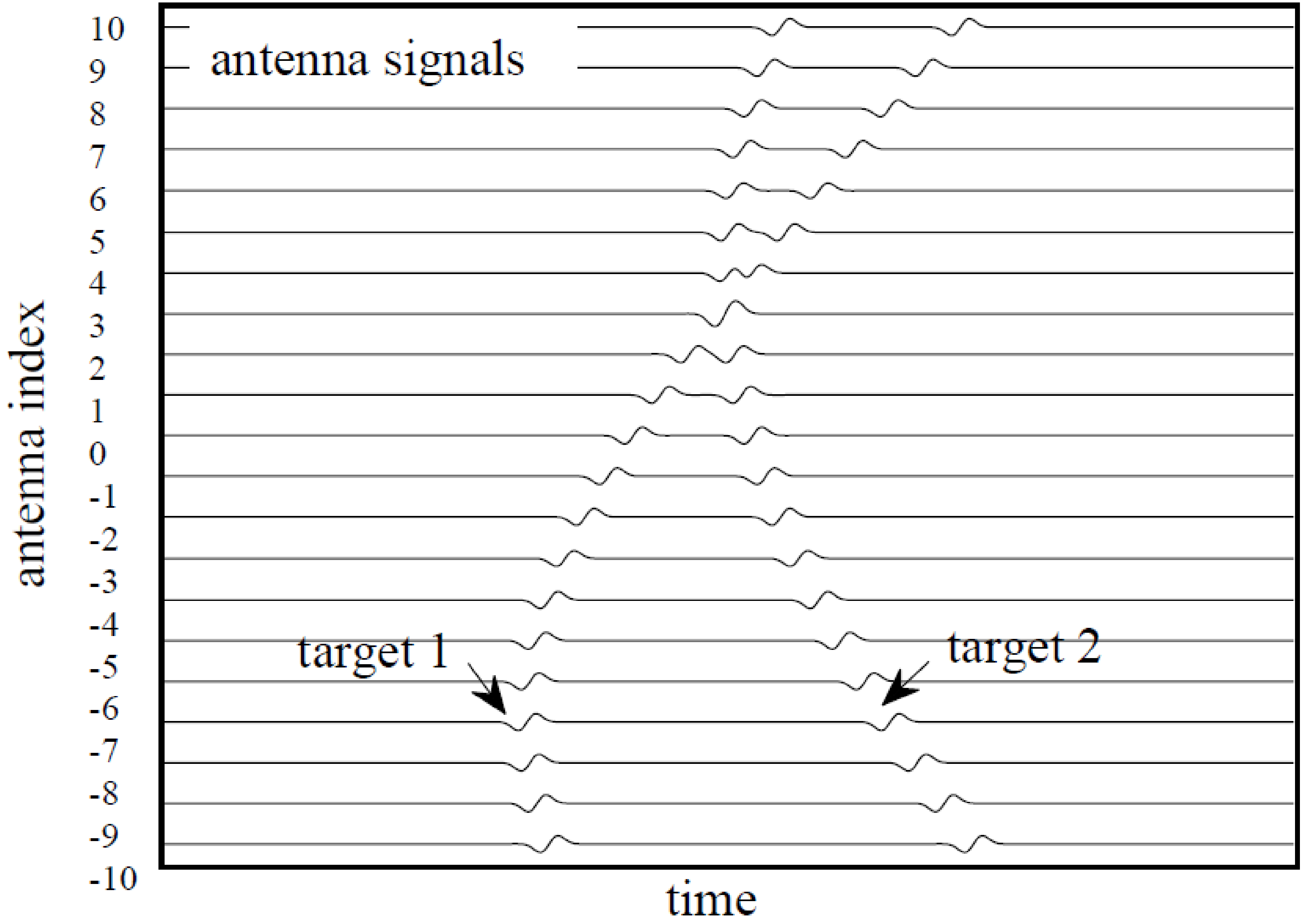

DAS: CONCEPTUAL EXAMPLE

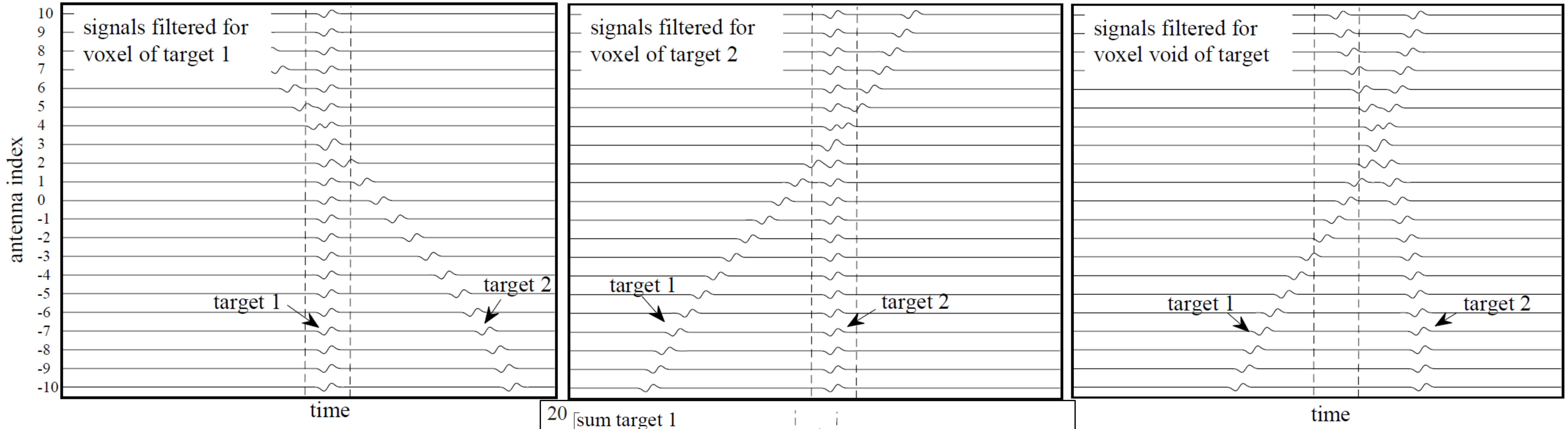

$$I(\mathbf{r}_1') \approx 2927$$

$$I(\mathbf{r}_2') \approx 2927$$

$$I(\mathbf{r}_{\text{void}}') \approx 14$$

$$y(\mathbf{r}',t)$$

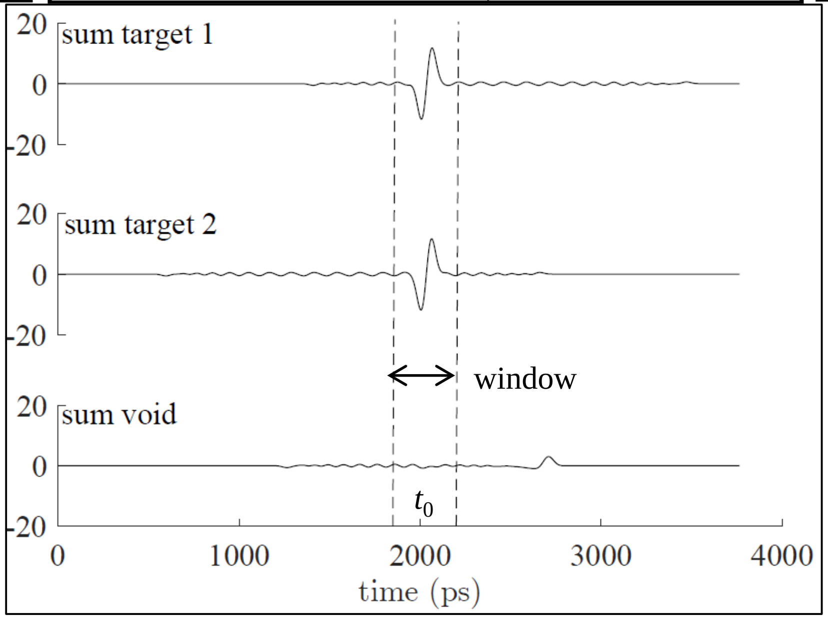

$$I(\mathbf{r}') = \int_t y_w^2(\mathbf{r}',t)\,dt$$

plot image

DAS: 2-D SIMULATION EXAMPLE

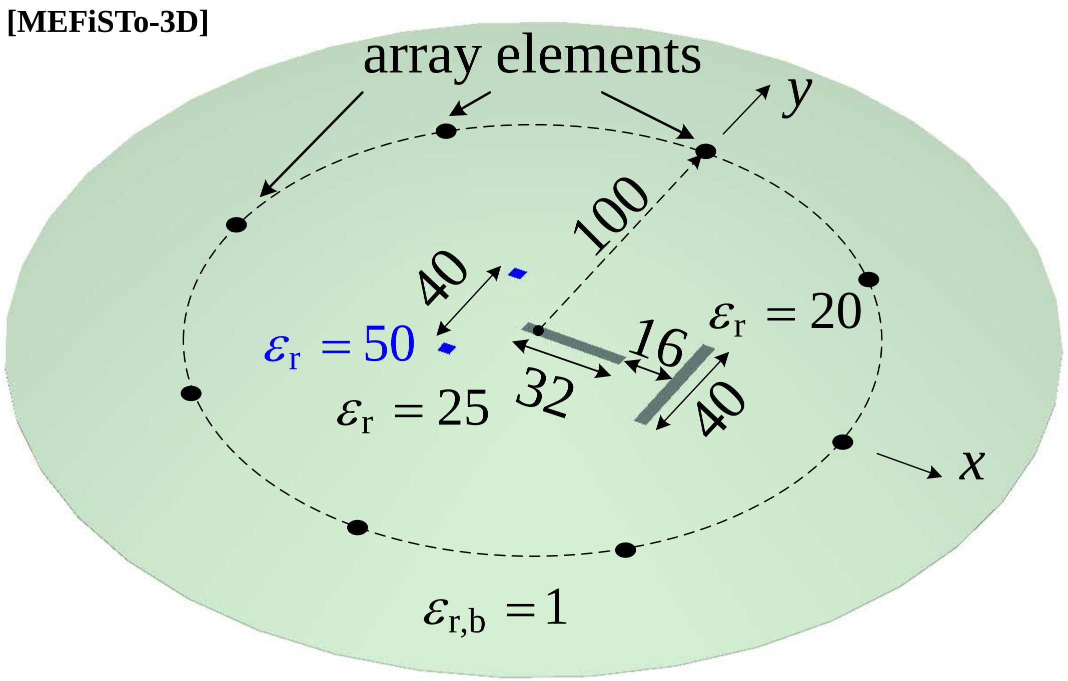

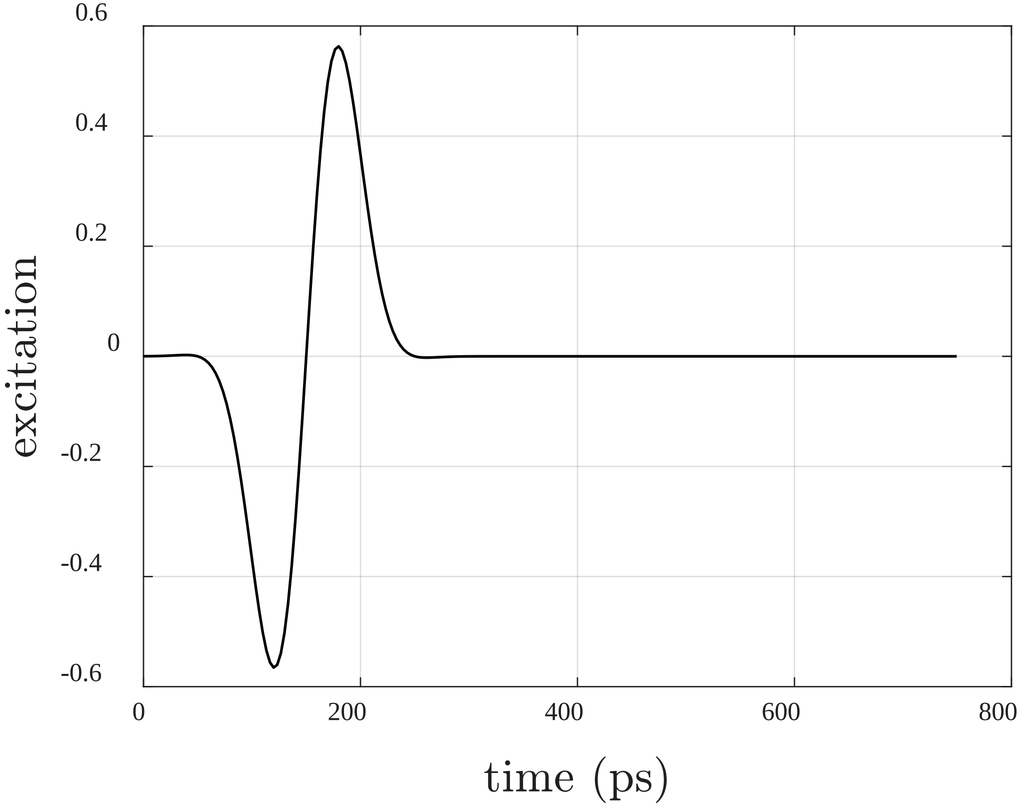

- 2-D simulation (TM$_z$ mode)
- point sources
- point probes recording $E_z(t)$

bandwidth at 3 dB
from 1.25 GHz to 8.75 GHz

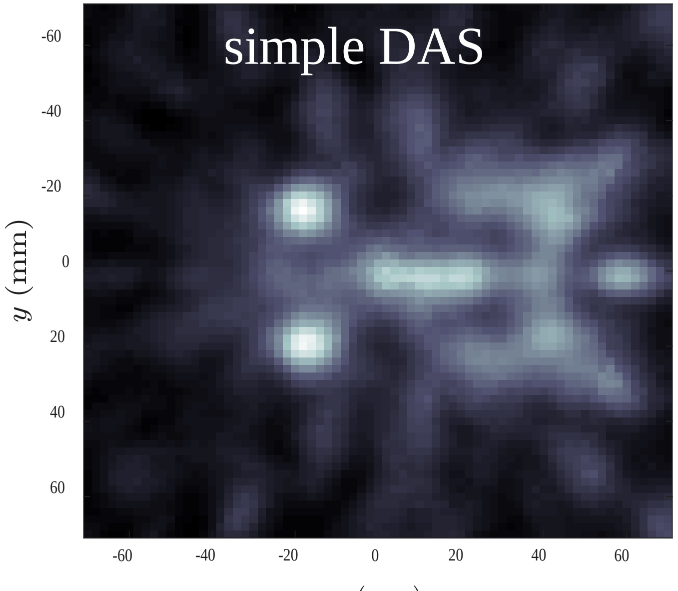

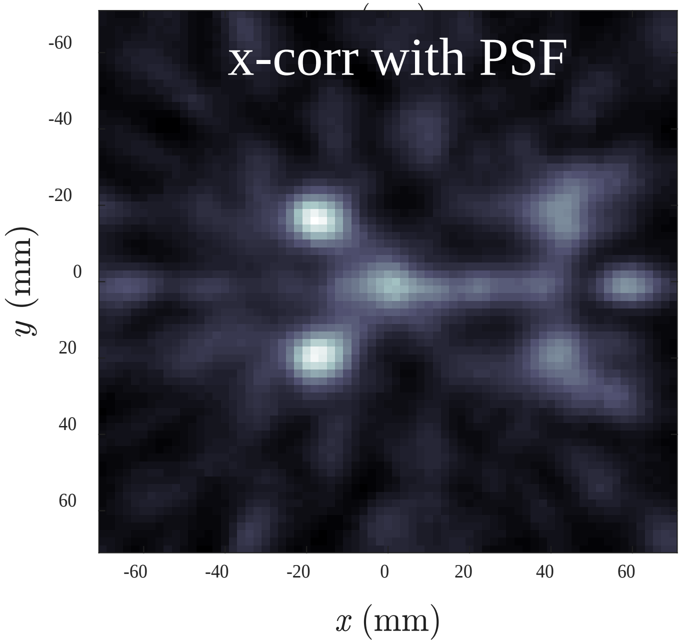

discussion

- *Why the simple DAS algorithm (PSF is a δ-function of time) performs similarly to the more sophisticated x-correlation with the actual simulated PSF?*
  - ➢ due to the point-like nature of the sources and probes
- *Why do we have so many artifacts?*
  - ➢ because the forward model does not take into account mutual coupling and scattering between close-by targets
  - ➢ the Tx total field is not the same as the Tx incident field (as the linearized model assumes) and these differences appear as spurious contrast (image artifacts)
  - ➢ because we have only 8 probes – incomplete data!

SUMMARY OF DAY TWO

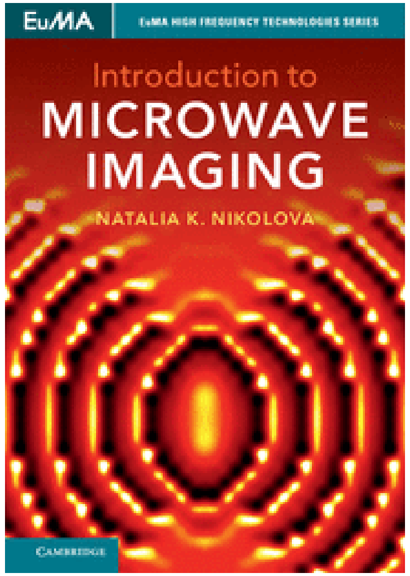

- real-time imaging methods provide an image within seconds of the data acquisition
- real-time methods substantially rely on linearized forward models
- there are 2 main types of real-time imaging methods
  - ➢ direct solution of the data equation (microwave holography)
  - ➢ cross-correlation with system PSF (scattered-power mapping & synthetic focusing)
- assumption of uniform or layered medium enables super-fast solution in Fourier space
- however, inversion in Fourier space has some "pitfalls" – we discuss those and the respective mitigation strategies during Day Three of this course

QMH, SPM codes available:
http://www.ece.mcmaster.ca/faculty/nikolova/IntroMicrowaveImaging/MatlabCodes/
We keep updating!


[worldartsme.com]

THANK YOU!